STOCHASTIC MODELLING OF PREDATOR-PREY DYNAMICS IN A THREE-PATCH ECOSYSTEM WITH OPTIMAL HARVESTING

Lucian Talu Mayabi

A Thesis Submitted in Partial Fulfillment for the Requirements of the Award of the Degree of Doctor of Philosophy in Applied Mathematics of Masinde Muliro University of Science and Technology

NOVEMBER, 2025

TITLE PAGE

DECLARATION

This thesis is my original work prepared with no other than the indicated sources and support and has not been presented elsewhere for a degree or any other award.

Signature..... Date .....

MAYABI LUCIAN TALU

SEA/H/01-70392/2022

CERTIFICATION

The undersigned certify that they have read and hereby recommend for acceptance of Masinde Muliro University of Science and Technology a research thesis entitled “Stochastic Modelling of Predator-Prey Dynamics in a Three-Patch Ecosystem with Optimal Harvesting”.

Signature..... Date.....

Dr. David Angwenyi

Department of Mathematics

Masinde Muliro University of Science and Technology.

Signature..... Date.....

Dr. Duncan Oganga

Department of Mathematics

Masinde Muliro University of Science and Technology.

COPYRIGHT

DEDICATION

This research thesis is dedicated entirely to my dad, Amukoa Mayabi and my late mum, Euphemia Mwachia.

ACKNOWLEDGEMENTS

First and foremost, I thank the Almighty God for the grace of good health during my thesis writing period. It is my sincere pleasure to express my utmost appreciation to Masinde Muliro University of Science and Technology for granting me an opportunity to undertake a Doctoral Programme in Mathematics Department. The successful development and completion of this thesis is highly attributed to the efforts and professional guidance of my able supervisors; Dr. David Angwenyi, and Dr. Duncan Oganga. I sincerely acknowledge with thanks the Department of Mathematics staff members, Masinde Muliro University of Science and Technology for their support during this study.

ABSTRACT

Predator-prey interactions play a pivotal role in shaping ecological dynamics, and understanding these interactions is critical for sustainable resource management and effective conservation. Existing literature predominantly focused on deterministic models incorporating optimum harvesting policy involving two ecosystems or less. Moreover, while stochastic models had been employed to account for randomness and uncertainty in ecological interactions, these studies were often limited to single-patch ecosystems. The stochastic dynamics of predator prey models involving more than two ecosystems had been given little attention in literature yet they are critical in conservation and resource management. Therefore, this research developed a stochastic predator-prey model with optimum harvesting for three patches namely "cages" which are within a lake, containing a predator-prey system involving large Nile perch as predators and smaller fish as prey. The dynamics of the prey population could transfer from one cage to the other. The study aims to investigate how randomness and harvesting controls affect population stability and sustainability. Stability analysis of the deterministic part was carried out in order to study the long term behaviour of solutions around equilibrium points. Stability analysis of the stochastic model was done using stochastic Lyapunov function method assessing its impact on the system dynamics. Numerical analysis was done to explain the analytic approach. From the results, when $e_i < 1$ (e_i is the predator's efficiency in converting prey into a new predator), the lyapunov function, $V(t)$, stays bounded indicating stochastic stability, and when $e_i > 1$, $V(t)$ grows without bound indicating that the system is unstable. An optimal control problem was formulated to derive harvesting functions that maximize resource utility while maintaining a sustainable ecosystem employing the Pontryagin's Maximum Principle. From Numerical simulation, prey populations remained viable when the harvesting rates were maintained below $\nu_1 = 0.02$, $\nu_2 = 0.02$, and $\nu_3 = 0.02$, and noise intensities were controlled at $\sigma = 0.10$, and $\sigma = 0.90$. The findings highlight the impact of human activities, particularly harvesting, on ecosystem balance. They also contribute to conservation biology, fisheries management, and mathematical ecology, providing insights for sustainable resource management and effective conservation strategies.

TABLE OF CONTENTS

LIST OF ABBREVIATIONS

MATLAB - Matrix Laboratory

ODE - Ordinary Differential Equation

SDEs - Stochastic Differential Equations

LIST OF FIGURES

LIST OF TABLES

CHAPTER ONE

INTRODUCTION

1.1 Background Information

In a natural ecosystem, when species live together, there is some biological interaction. Predation is a biological process where the predator feeds on the prey [7, 14, 28]. Predator-prey interactions are fundamental to ecological systems [33]. The relationship between species influences population dynamics, community structure, and overall ecosystem health. Classical models, such as the Lotka-Volterra equations, have provided significant insights into the predator-prey interactions, illustrating cyclical patterns of population growth and decline [28]. However, real-world ecosystems exhibit complexities that are often not captured by deterministic models, including spatial heterogeneity and stochastic fluctuations.

Understanding predator-prey dynamics is vital for predicting the effects of disturbances and implementing effective conservation strategies as well as sustainable management practices [26]. Effective management of fisheries relies on accurate models that predict the outcomes of various interventions, such as harvesting or habitat modifications [11]. Sustainable harvesting strategies are particularly important in ensuring that economic benefits do not come at the cost of long-term ecological damage [13].

Harvesting involves the process of removing some members of a population in an ecosystem [29]. Harvesting can either be based on yield or effort and at each time varying the dynamics. In [6], constant yield harvesting arises in situations when quotas are set, such as through permits, as in some cases of species dictated by seasonal variations, or by agreement. The logistic equation with harvesting, in which N(t) represents the stock level (population size or density) of the species (usually the prey) at time t, takes the form;

$$\frac{dN}{dt} = N(r - bN) - \nu \tag{1.1}$$

where ν is the constant harvesting rate, r is the intrinsic growth rate of the population, and b is a constant related to density dependence and the carrying capacity. In [3, 8], constant effort harvesting assumes that the catch per unit effort applied, is proportional to the stock levels. An application to fisheries depicts that the number of fish N(t), caught per unit time is proportional to the effort E. The effort is measured in terms of number of boats used, how far into the lake the fisherman goes, how strong the boat used is among others. The underlying dynamics are represented by:

$$\frac{dN}{dt} = rN(1 - \frac{N}{K}) - qEN \tag{1.2}$$

where qEN is the harvesting rate, q represents the catchability, E is the fishing effort, r is the intrinsic growth rate of the population, and N is the stock level.

Overharvesting (either of prey or predator) makes the population go to extinction which can be avoided by setting a fixed fishing effort [52]. When population is large, a fixed effort gives a large harvest. When the population declines, the fixed effort takes a smaller harvest and allows recovery. According to [30], overfishing is a universal threat affecting marine species and therefore there is need for urgent approaches to minimize mortality of the threatened species to ensure a sustainable catch.

Ecosystems are often spatially heterogeneous, comprising multiple patches with distinct environmental conditions [19]. The movement of species between these patches can significantly impact population dynamics. Investigating multi-patch ecosystems is crucial for capturing the complexity of real world ecological systems. In [4, 5, 12, 36, 46], harvesting done in preda-

tor prey models has been discussed in different dimensions. Harvesting has a strong impact on dynamic evolution of a population and therefore, there has been a considerable interest in the modeling of biological resources [26]. In these models [42, 43, 44, 45], the harvesting effort is considered to be a dynamic variable; several kinds of harvesting policies are utilized to study the dynamical behavior of the model system.

Stochastic modeling involves incorporating randomness or uncertainty into mathematical models, and are essential for providing a more realistic representation of ecological processes [17]. In ecological contexts, stochasticity can arise from environmental variability, demographic fluctuations, or other unpredictable factors [41]. A research was done on stochastic stability of a fishery model with optimal harvesting policy in [18]. Another research was done on fishery resource management with migratory prey harvesting in two zones-delay where a stochastic approach was considered [31]. The study examined a two-zone aquatic ecosystem in which the prey randomly switches between two zones and both predators and prey have access to the zones or patches. In each zone, the growth of prey in the absence of a predator was thought to be logistic. Random environmental disturbances were approximated using additive white noise perturbations that followed a Gaussian process. It was found that when the population variance is high, the system is likely to be more unstable in the respective area. However, the model considers only two zones for migratory prey harvesting, which may be an oversimplification. Real-world fisheries often involve more complex spatial dynamics and multiple interacting zones. Extending the model to include more zones could provide a more realistic and applicable framework for resource management.

In recent years, cage farming has been on the rise especially in L. Victoria and has experienced significant growth as an innovative and efficient method for aquaculture. Despite its increasing popularity, there remains a notable gap in comprehensive studies addressing the ecological, biological, and economic implications of cage farming. Specifically, the dynamics of predator-prey interactions within these confined environments, optimal harvesting strategies, and the stochas-

tic effects of environmental variability are areas that require further investigation. This lack of in-depth research highlights the need for more focused studies to develop sustainable practices and optimize production, ensuring the long-term viability of cage farming systems. Recently, a research on cage farming has been done where critical bait casting threshold of cage culture in open advective environments [39]. While the methodology is robust, it would be beneficial to include a more detailed description of the experimental setup, including the size and type of cages, species of fish used, and the duration of the study.

Optimal harvesting involves determining the best practices for extracting resources to maximize yields while ensuring sustainability [10]. A predator-prey model with optimum harvesting consisting of two zones, free fishing and prohibited zones, was done [40]. It was discovered that in the free fishing zone, there is a particular value of harvesting efforts for the populations of predators and prey that optimizes the net revenue's present value. In addition, neither the prey nor the predator populations in the two zones will go extinct. The study does, however, use the assumption that predator and prey populations in the free fishing zone will always be harvested. In actuality, a variety of factors, including market demand, fishing equipment, and legislative changes, can cause variations in harvesting efforts. Additionally, the migration dynamics between free fishing and reserve zones are simplified. In natural ecosystems, migration patterns can be influenced by a variety of ecological and environmental factors that are not accounted for in the model.

Existing literature predominantly focused on deterministic models incorporating optimum harvesting policy involving two ecosystems or less. Moreover, while stochastic models have been employed to account for randomness and uncertainty in ecological interactions, these studies are often limited to single-patch ecosystems. The stochastic dynamics of predator prey models involving more than two ecosystems has been given little attention. Therefore, this research developed a stochastic predator prey model with optimum harvesting for three ecosystems namely "cages" which are within a lake. A three-patch system provides a richer model structure that cap-

tures spatial heterogeneity and inter-patch movement, yet still allows for tractable mathematical analysis and meaningful interpretation of equilibrium and stability results. In fisheries management, this framework enables the examination of how migration, harvesting and environmental variability influence overall population sustainability.

1.2 Statement of the Problem

Predator-prey models predict a broad range of results based on the nature of interactions between the predators, the prey and their ecosystems. Whereas ecosystems are composed of various interacting components, predator-prey interactions across patches are inadequately studied especially when they are exposed to stochastic effects and optimality in harvesting. Although there has been a great advancement in the modeling of predator-prey dynamics, a general model, which integrates both stochastic processes and harvesting effects in a multitude of patches, has not yet been developed. The gap in this research was that a robust stochastic model that put into consideration the complexities of predator prey interactions and optimal harvesting strategies in a three patch ecosystem was developed. Understanding these dynamics was crucial for informing sustainable management practices and conservation efforts in ecosystems characterized by spatial heterogeneity.

1.3 Objectives of the Study

1.3.1 Main objective

The main objective of this study was to develop a stochastic predator-prey model for a three-patch ecosystem with optimal harvesting.

1.3.2 Specific objectives

(i) To develop a stochastic predator-prey model for a three-patch ecosystem.

(ii) To carry out stability analysis of both deterministic and stochastic part of the model in

order to study the long-term behaviour of solutions.

(iii) To formulate the optimal harvesting function for the dynamics.

(iv) To simulate and analyze both deterministic and stochastic model dynamics.

1.4 Justification of the Study

Harvesting in predator-prey models regulates population growth. Harvest rate has a strong influence on the dynamic growth of the population. Overharvesting of the prey makes the prey population go to extinction. With ecosystems worldwide facing unusual challenges due to overharvesting, there is a pressing demand for expressing mathematical models that capture the complexity of these interactions. The study focused on a three-patch ecosystem, combined with the incorporation of stochastic elements and optimum harvesting strategies, and this offered a unique perspective on the interplay between predator and prey species. The three patch model is relevant as it enables the study of movement and spatial heterogeneity between patches, which is more realistic in ecology. The study contributes valuable information that can be used in the sustainable management of forests through treating the effects of harvesting. Moreover, the results are applicable in practice to the fisheries policy management, in which they may be used to formulate the evidence-based harvesting limits (in which the harvesting effort must be based on the real-time population in order to avoid over-harvesting at the time of low prey-population) to maintain the ecological balance and to support the economic productivity.

1.5 Significance of the Study

Combining the intricate predator-prey interactions in a three-patch ecosystem and adding both the stochastic components and optimal harvesting techniques, the studies do not only bring value to ecological studies but also resolve some of the most critical questions on the effective conservation and sustainable management of resources. Upon the analysis of the proposed stochastic predator-prey mathematical model with optimum harvesting, the findings highlight the impact of human activities, particularly harvesting, on ecosystem balance. They also contribute to conser-

vation biology, fisheries management, and mathematical ecology, providing insights for sustainable resource management and effective conservation strategies.

1.6 Methods

1.6.1 Model Development

A system of differential equations was formulated to model the interactions between prey and predator populations across three spatially distinct but interconnected patches. Each patch is represented as a fish cage with mesh boundaries that allow the migration of prey fingerlings. The deterministic part of the model comprises logistic growth for prey, predator-prey interactions, harvesting, and inter-patch migration. Stochasticity was introduced through white noise terms: $d\eta_t$, $d\xi_t$, and $d\varepsilon_t$, to capture the unbounded variations in the population over time resulting in a system of stochastic differential equations (SDEs).

1.6.2 Model Analysis

The developed model was analysed where;

(i) Stability analysis of the deterministic part of the model was carried out in order to study the long term behaviour of solutions about all the equilibrium points with the help of MATLAB software. Local stability of the equilibria was analyzed using linearization and Jacobian matrix techniques.

(ii) Stability analysis of the stochastic model was carried out using stochastic Lyapunov function [50] assessing its impact on the system dynamics. A suitable Lyapunov candidate function $V(t)$ was constructed and stability was determined by evaluating the sign of the expected derivative of $V(t)$ along the solution trajectories.

(iii) An optimal control problem was formulated to derive harvesting functions that maximize resource utility while maintaining a sustainable ecosystem employing the Pontryagin's

Maximum Principle [25] to derive the necessary conditions for optimal control, including the Hamiltonian, adjoint equations, and optimality conditions.

(iv) Numerical simulations were carried out to analyze both deterministic and stochastic model dynamics using Runge-Kutta method (RK45) and Euler-Maruyama Scheme respectively with the help of Python software illustrating population trajectories under different harvesting rates and noise intensities. Time evaluation graphs were generated for both deterministic and stochastic cases, providing visual insights into system behavior.

CHAPTER TWO

LITERATURE REVIEW

2.1 Introduction

In this chapter, we present a review of existing literature related to predator-prey modeling with and without harvesting. In Section 2.2, we introduce the classical predator-prey models. Section 2.3 reviews deterministic models that incorporate harvesting strategies. Section 2.4 discusses stochastic predator-prey models with harvesting. In Section 2.5, a comparative discussion is given on both stochastic and deterministic models used to study predator-prey dynamics under harvesting conditions. Section 2.6 highlights the research gap and the motivation for the study.

2.2 Classical Predator-Prey Model

The Lotka-Volterra model is an example of a classical predator-prey model which represents the interaction of the predator and the prey species that were initially proposed by Alfred J. Lotka [22] in 1925 and Vito Volterra [48] in 1926, both in the context of competing species. Lotka first suggested a model for the study of a plant species and a herbivorous animal species. Later, he produced an application for the study of the dynamics of a predator-prey system. In order to explain the findings about the rise in the proportion of predatory fish captured during World War I, Volterra simultaneously examined the same model. Volterra was interested in researching the circumstance because the fishing effort had decreased during those years, making this fact seem perplexing. Volterra proposed a straightforward system of ordinary differential equations to describe this pattern. The model describes the dynamics of biological systems in which two species interact, one as a predator and the other as prey. The Lotka-Volterra equations consist of two first-order, non-linear differential equations;

$$\begin{aligned} \frac{dx}{dt} &= \alpha x - \beta xy, \\ \frac{dy}{dt} &= \delta xy - \gamma y. \end{aligned} \tag{2.1}$$

where x represents the prey population, y represents the predator population, α is the maximum prey per capita growth rate in the absence of predators, β is the effect of the presence of predators on the prey death rate, γ is the predator's per capita death rate, δ is the effect of the presence of prey on the predator's growth rate. All parameters are positive and real. The classical Lotka-Volterra predator-prey model, while foundational in theoretical ecology, is oversimplified and has unrealistic assumptions. It assumes that the environment will always be homogeneous (single-patch), this may not be realistic since the environment is heterogeneous (many patches) and its connected by a diffusion-like process referred to as migration. Additionally, it ignores environmental variability, demographic stochasticity, and spatial structure, which are crucial for capturing the complexity of real-world ecosystems. These limitations highlight the need for more refined models that incorporate stochastic influences, spatial heterogeneity, and adaptive behaviors to better reflect the dynamics of natural predator-prey interactions.

2.3 Deterministic Predator-Prey Models with Harvesting

A harvested predator-prey system incorporating prey migration was done [46]. This work presents analysis of the effect of harvesting efforts and prey refuge on the prey–predator system. The model is described by the following differential equations;

$$\begin{aligned} \frac{dx}{dt} &= \alpha x(1-\frac{x}{K}) - \frac{\beta(1-m)xy}{1+\alpha(1-m)x} - q_1E_1x, \\ \frac{dy}{dt} &= -\gamma y + \frac{c\beta(1-m)xy}{1+\alpha(1-m)x} - q_2E_2y. \end{aligned} \tag{2.2}$$

where x and y denote the prey and predator population, respectively, at any time t, α represents

the intrinsic growth rate of the prey, k is the carrying capacity of the prey in the absence of predator and harvesting, γ is the death rate of the predator, E_1 and E_2 denote the harvesting efforts for the prey and predator, respectively. From the model, Mite prey–predator interactions often exhibit spatial refugia which afford the prey some degree of protection from predation and reduce the chance of extinction due to predation. Analysis showed that using harvesting as a control can break down the cyclic behaviour of the given system and this will drive it back to the required state. While the study suggests that harvesting can control cyclic behavior, it does not thoroughly address the potential long-term ecological consequences of harvesting. Overharvesting can lead to population declines and disrupt ecosystem balance. A more comprehensive analysis of sustainable harvesting practices is needed.

A study on the predator–prey interaction with harvesting: mathematical study with biological ramifications was later done in [38]. In this paper, an assumption made was that the predator population is subjected to harvesting. The harvesting effort was varied from very low, low, intermediate and high rates and at each time comparing the populations of both the predator and the prey. When predator is harvested at a lower rate, predator consumes all the preys which forces prey population to go to extinction. The model is described by the following differential equations;

$$\begin{aligned} \frac{dx}{dt} &= rx(1-\frac{x}{K})-\frac{\alpha xy}{\alpha y+x}, \\ \frac{dy}{dt} &= \frac{\alpha b_0 xy}{\alpha y+x}-d_0 y-Ey. \end{aligned} \tag{2.3}$$

where x(t) and y(t) denote the prey and predator population, respectively, at any time t, the prey population grows logistically to its carrying capacity, K, with intrinsic growth rate, r, in absence of predator, d_0 and b_0 denote the food-independent death rate and the conversion efficiency of predator respectively. Analysis showed that harvesting effort and predator's attack rate may be used as control parameters for the system. The study assumes that only the predator population

is subjected to harvesting. This assumption may not fully capture the complexity of real-world ecosystems where both predators and prey could be harvested, either intentionally or unintentionally. This simplification may limit the applicability of the findings. Additionally, the model does not account for prey refugia or migration, which are important ecological factors that can significantly impact predator-prey dynamics. These factors could provide prey with means of escape and survival, thereby altering the outcomes predicted by the model.

An advancement of the research was done on the comparison and analysis of two forms of harvesting functions in the two-prey and one-predator model [21]. It considered two teams of prey interacting with one team of predators and the harvesting functions for two prey species adopting the traditional form (human's harvesting and the internal reproduction of a biological system itself take place simultaneously) and the new form (in which the number of species at the next moment is the change of the part which is not harvested by humans) for prey one and prey two respectively. The model is described by the following differential equations;

$$\begin{aligned}
\frac{dx_1}{dt} &= r_1 x_1\left(1-\frac{x_1}{K_1}\right)-\beta x_1 y - q_1 E_1 x_1 - \sigma x_1(x_2 - q_2 E_2 x_2) \\
&\triangleq x_1 f_1(x_1, x_2, y, E_1, E_2), \\
\frac{dx_2}{dt} &= r_2(x_2 - q_2 E_2 x_2)\left(1-\frac{x_2 - q_2 E_2 x_2}{K_2}\right)-\beta_2(x_2 y - q_2 E_2 x_2)y \\
&\quad -\sigma x_1(x_2 - q_2 E_2 x_2) \\
&\triangleq (1-q_2 E_2)x_2 f_2(x_1, x_2, y, E_2), \\
\frac{dy}{dt} &= \eta_1\beta_1 y + \eta_2\beta_2(x_2 - q_2 E_2 x_2)y - my \\
&\triangleq y g(x_1, x_2, E_2),
\end{aligned} \tag{2.4}$$

here,

$$\begin{aligned} f_1(x_1,x_2,y,E_1,E_2) &= r_1(1-\frac{x_1}{K_1})-\beta x_1 y - q_1 E_1 - \sigma x_2(1-q_2E_2), \\ f_2(x_1,x_2,y,E_2) &= r_2[1-\frac{(1-q_2E_2)x_2}{K_2}]-\beta_2 y - \sigma x_1, \\ g(x_1,x_2,E_2) &= \eta_1\beta_1 x_1 + \eta_2\beta_2(1-q_2E_2)x_2 - m. \end{aligned} \tag{2.5}$$

where r_i represents the intrinsic growth rate of prey x_i (i = 1,2), K_i is the carrying capacity of prey x_i, d is the per capita death rate of the predator y, E_i is the harvesting effort of the prey x_i, and q_i is the catchability coefficient of the prey x_i. The analysis showed that by capturing and training species continuously, the harvesting may promote population growth and reproduction. However, the model simplifies the interaction dynamics by focusing on two prey species and one predator. In natural ecosystems, interactions are typically more complex, involving multiple predators, prey, and other environmental factors that can influence outcomes.

Optimal Harvesting Policy of Predator-Prey Model with Free Fishing and Reserve Zones was done [40]. The ecosystem's prey population dynamics shift from the unrestricted fishing zone to the forbidden zone, where the fish population was shielded from overexploitation by regulating the tax, and vice versa. The populations of predators and prey in the free fishing zone are then continuously fished or exploited. The following differential equations describe the model;

$$\begin{aligned} \frac{dx}{dt} &= rx(1-\frac{x}{K})-a_1x+a_2y-a_3x-\alpha xz-q_1E_1x, \\ \frac{dy}{dt} &= sy(1-\frac{y}{L})+a_1x-a_2y-a_4y, \\ \frac{dz}{dt} &= m\alpha xz-kz-q_3E_3z. \end{aligned} \tag{2.6}$$

where r is the intrinsic growth rate of the prey population in the free fishing zone; z(t) is the size of the predator population in the free fishing zone at time t; K is the carrying capacity of the ecosystem for the prey population; L is the carrying capacity of the ecosystem for the prey

population in the prohibited zone; a_3, a_4, and k are the mortality rates for the prey in the free fishing zone, the prey in the prohibited zone, and predator in that order, q_1 and q_3 indicate the catchability coefficient for the prey and predator populations, respectively; E_1 and E_3 indicate the harvesting efforts; a_1 indicates the migration rate from the prey in the free fishing zone to the prey in the prohibited zone; and a_2 indicates the migration rate from the prey population in the prohibited zone to the prey population in the free fishing zone. The results of the analysis indicated that the populations that are harvested in the free fishing zone yield the most profit; the predator and prey populations in the free fishing zone have a particular value of harvesting efforts that maximizes the net revenue's present value while preventing the extinction of the prey and predator populations in both zones. The study does, however, use the assumption that predator and prey populations in the free fishing zone will always be harvested. In actuality, a variety of factors, including market demand, fishing equipment, and legislative changes, can cause variations in harvesting efforts. It also simplifies the migration dynamics between conservation zones and free fishing areas. Numerous biological and environmental elements that are not included in the model can affect migration patterns in natural ecosystems.

Optimal harvesting of a Predator-Prey system with marine reserve was done [24]. This study formulates an optimal control problem involving a predator-prey model with partial harvesting of the prey species. Some quantity of fish stock is made available for harvesting while the remaining put in an adjacent marine reserve. The model is described by the following differential equations;

$$\begin{aligned} \frac{dx}{dt} &= rx(1-\frac{x}{K}) - uqEx, \\ \frac{dE}{dt} &= uqE(x-a). \end{aligned} \tag{2.7}$$

where qEx is the harvesting rate, uqEx is harvesting function is modified by incorporating a marine reserve, ux is the quantity of fish available for harvesting, (1 - u)x is the quantity of fish in the adjacent marine reserve, x(t) denotes the size of fish population (or biomass) – the prey

– and E(t) represents the fishing effort and may be considered as the size of the 'population' of fishermen–the predator (fishing is viewed as a form of predation). From the analysis, the study revealed that the fishery is sustainable even without the imposition of a reserve area when the critical biomass level is at least 50% of the carrying capacity. However, the study appears to rely on several assumptions that might limit the applicability of its findings. For instance, the assumption that fish stock is uniformly distributed and the harvesting effort is evenly applied may not reflect real-world complexities such as spatial heterogeneity and variable fishing efforts.

2.4 Stochastic Predator-Prey Models with Harvesting

A study on optimal harvest of a stochastic predator-prey model in [16]. The main idea was to show the permanence of hybrid prey-predator system when both white and color noises are taken into account. The stochastic dynamics of the system subject to harvesting takes the form;

$$\begin{aligned} dx(t) &= x(t)[a_1 - E_1 - b_1 x(t) - c_1 y(t)]dt + \sigma_1 x(t) dB_1(t), \\ dy(t) &= y(t)[a_2 - E_2 - b_2 y(t) + c_2 x(t)]dt + \sigma_2 y(t) dB_2(t). \end{aligned} \tag{2.8}$$

where x(t), y(t) represent the prey and the predator populations at time t, respectively. From analysis, optimal management of renewable resources has a direct relationship to sustainable development. When population system is subject to exploitation, it is important and necessary to discuss the optimal harvesting effort and the corresponding maximum sustainable yield. Population systems are often subject to environmental noise and it is necessary to reveal how the noise affects the population systems. The researcher states that the work was just an attempt to carry out the study of optimal harvest policy of population system in a stochastic setting. However, the research appears to be more theoretical, incorporating case studies could strengthen the findings by demonstrating how the theoretical models apply to real-world scenarios. Additionally, the researcher mentions that this work is an attempt. It would be beneficial to explicitly state the

limitations of the current study and suggest directions for future research. This can help frame the study within the broader context of ongoing research efforts.

An advancement on optimal harvesting policy for a stochastic predator–prey model was later done in [27]. The study's model was predicated on the ideas that only the prey population is exploited and that environmental variables, such as changes in purchasing power, have an impact on harvesting effort. The stochastic system that follows was taken into consideration;

$$\begin{aligned} dN_1(t) &= N_1(t)(r_1 - h - a_1 N_1(t) - bN_2(t))dt + \rho N_1(t)dW(t), \\ dN_2(t) &= N_2(t)(-r_2 + a_2 N_1(t))dt. \end{aligned} \tag{2.9}$$

where N_1 and N_2 are the sizes of the prey and predator respectively, r_i, a_i and b are positive numbers where i = 1,2, h is the harvesting effort, W(t) is a Wiener process defined on a complete probability space (Ω, Σ, μ) and ρ stands for the intensity of the environmental noise. The main aim as to why a stochastic approach was employed was to obtain the optimal harvesting effort such that the expectation of sustained yield is maximum and the predator population does not go to extinction. The study's analysis provided adequate and essential criteria for the presence of the best harvesting approach, the best harvest effort, and the highest anticipated sustainable yield. The researcher does point out a flaw in the methodology, though. Since their findings were predicated on the explicit solution of the model's Fokker-Planck equation, their method is invalid for other stochastic models if the related Fokker-Planck equation cannot be solved explicitly.

A study was done on stochastic predator–prey model with Allee effect on prey [32]. A system of stochastic differential equations describes the dynamics under the assumption that environmental randomness is represented by noise terms affecting each population (taking into account a term that expresses the variability of both species' growth rates due to external, unpredictable events), and that the intensities of these perturbations are proportionate to the size of each species' popu-

lation. The model takes into account a set of stochastic differential equations with the structure;

$$\begin{aligned} dx &= [r(1-\frac{x}{k})x - \frac{mx}{x+b} - \frac{qxy}{x^2+a}]dt + \sigma_1 x dW_1(t), \\ dy &= [s(1-\frac{y}{nx})y]dt + \sigma_2 y dW_2(t). \end{aligned} \tag{2.10}$$

where x(t) and y(t) denote prey and predator densities, respectively, as functions of time t, s is the intrinsic growth rate of the predator, $\frac{qxy}{x^2+a}$ is the functional response function, $\frac{m}{x+b}$ is the allee effect function, W(t) = $(W_1(t), W_2(t))$ is a two-dimensional Brownian motion and parameters σ_1, σ_2 represent the intensity of the perturbation. Analysis reveals that a variety of biological processes can interact with the Allee effect and ambient noise, making the identification of their effects on species behavior, conservation, and reproduction a crucial objective for the population dynamics community. Future research on the analysis of more general stochastic perturbations—which might even take random factors into account—is suggested by the work. However, considering other ecological interactions, such as predation, and their stochastic effects could be valuable extensions of the current work.

A research was done on fishery resource management with migratory prey harvesting in two zones-delay where a stochastic approach was considered [31]. The study examined a two-zone aquatic ecosystem in which the prey randomly switches between two zones and both predators and prey have access to the zones or patches. In each zone, the growth of prey in the absence of a predator was thought to be logistic. The following system of four non-linear ordinary differential equations is the stochastic model of a prey-predator fishery resource;

$$
\begin{aligned}
x'(t) &= \phi_1(x,z)x + \sigma_2 y + \beta_1 \xi_1(t), \\
y'(t) &= \sigma_1 x + \phi_2(y,w)y + \beta_2 \xi_2(t), \\
z'(t) &= \phi_3(x,z) + \beta_3 \xi_3(t), \\
w'(t) &= \phi_4(y,w) + \beta_4 \xi_4(t).
\end{aligned} \tag{2.11}
$$

here,

$$
\begin{aligned}
\phi_1(x,z) &= r - \sigma_1 - q_1 E_1 - m_1 z - (\frac{rx}{K}), \\
\phi_2(y,w) &= s - \sigma_2 - q_2 E_2 - m_2 w - (\frac{sy}{L}), \\
\phi_3(x,z) &= \alpha_1 z - (\frac{\alpha_1 z^2}{\gamma_1 x}), \\
\phi_4(y,w) &= \alpha_2 w - (\frac{\alpha_2 w^2}{\gamma_2 y}).
\end{aligned} \tag{2.12}
$$

In patch-1, E_1, K, x(t), z(t), γ_1, m_1, q_1, r, The biomass density of prey species, predator species, fish population harvesting effort, carrying capacity of prey species, equilibrium ratio of prey to predator biomass, prey mortality rate from predation, catchability coefficient, intrinsic growth rates of prey species, and intrinsic growth rates of predators are all represented by α_1. The symbols y(t), w(t), E_2, L, γ_2, in patch-2 m_2, q_2, s, α_2 for the prey species' biomass density, the predator species' biomass density, the effort made to reduce the fish population, the prey species' carrying capacity, the equilibrium ratio of prey to predator biomass, the prey mortality rate as a result of predation. The following are shown: catchability coefficient, intrinsic growth rate of prey species, intrinsic growth rate of predator species, and catchability coefficient, respectively. The migration rates from patch-1 to patch-2 and vice versa are represented by σ_1 and σ_2. The noise amplitude on the species prey1, prey2, predator1, and predator2 is represented by β_i, where i=1,2,3,4. $\xi(t) = [\xi_1(t), \xi_2(t), \xi_3(t), \xi_4(t)]$ is a Gaussian white noise process in four dimensions with a mean of 0.. It was found that when the population variance is high, the system is likely to be more unstable in the respective area. However, the model considers only two zones for mi-

gratory prey harvesting, which may be an oversimplification. Real-world fisheries often involve more complex spatial dynamics and multiple interacting zones. Extending the model to include more zones could provide a more realistic and applicable framework for resource management.

2.5 Stochastic and Deterministic Models of Predator-Prey Dynamics with Harvesting

A research on deterministic and stochastic prey–predator model for three predators and a single prey was done [51]. The interaction between three predators and a single prey was investigated, and the impact of harvesting on the three predators was studied. The models for the predator-prey dynamics are;

$$\begin{aligned}
\frac{dx}{dt} &= rx(1-\frac{x}{k}) - \beta_1 xy - \beta_2 xz - \frac{\beta_3 xw}{a+x}, \\
\frac{dy}{dt} &= m_1 xy + \delta yz - \mu_1 y - q_1 Ey, \\
\frac{dz}{dt} &= m_2 xz - \delta yz - \mu_2 z - q_2 Ez, \\
\frac{dz}{dt} &= \frac{m_3 xw}{a+x} - \mu_3 Ew.
\end{aligned} \tag{2.13}$$

$$\begin{aligned}
dx &= (rx(1-\frac{x}{k}) - \beta_1 xy - \beta_2 xz - \frac{\beta_3 xw}{a+x})dt + \sigma_1 x dW_1, \\
dy &= (m_1 xy + \delta yz - \mu_1 y - q_1 Ey)dt + \sigma_2 y dW_2, \\
dz &= (m_2 xz - \delta yz - \mu_2 z - q_2 Ez)dt + \sigma_3 z dW_3, \\
dz &= (\frac{m_3 xw}{a+x} - \mu_3 Ew)dt + \sigma_4 w dW_4.
\end{aligned} \tag{2.14}$$

Equations (2.13) and (2.14) represent the deterministic and stochastic models respectively where x is the population size of the single prey species, and y,z,w is the population size of the three predators, β_i (i=1,2,3) denote the predation rates of the first, second, and third predators on the prey, respectively, δ denotes the rate at which the first predator preys on the second preda-

tor; q_i (i=1,2,3) indicates the catchability constants; E stands for the harvesting effort; and W_i (i=1,2,3,4) are independent standard Brownian movements. Analysis revealed that harvesting can regulate population dynamics. The local and global dynamics of the prey-predator system were significantly influenced by the harvesting rates of the three predator species. They can drive the deterministic system to the desired state by stopping its oscillating behavior. Even though studying three predators is more complicated than single predator models, if all other species in the ecosystem are disregarded, interactions may still be oversimplified. This study may not adequately represent the many species and intricate food webs found in real ecosystems.

A study on deterministic and stochastic study of an eco-epidemic predator-prey model with non-linear prey refuge and predator harvesting was done [35]. The model system includes non-linear prey refuges, harvesting in the predator, and assumes that the predator population preys on both prey populations following Holling type I functional response [37]. The model is formulated on assumptions that the predator population consumes the two prey populations according to Holling type I scheme with different searching rates and there is a constant rate of harvesting of the predator species. The models for the predator-prey dynamics are;

$$\begin{aligned}
\frac{dx}{dt} &= rx(1-\frac{x}{k}) - \sigma xy - m(1-\delta_1 z)xz, \\
\frac{dy}{dt} &= \sigma xy - n(1-\delta_2)yz - d_1 y, \\
\frac{dz}{dt} &= e_1 m(1-\delta_1 z)xz + e_2 n(1-\delta_2 z)yz - (d_2+h)z.
\end{aligned} \tag{2.15}$$

$$\begin{aligned}
dx &= (rx(1-\frac{x}{k}) - \sigma xy - m(1-\delta_1 z)xz)dt + \sigma_1 x dw_1(t), \\
dy &= (\sigma xy - n(1-\delta_2)yz - d_1 y)dt + \sigma_2 y dw_2(t), \\
dz &= (e_1 m(1-\delta_1 z)xz + e_2 n(1-\delta_2 z)yz - (d_2+h)z)dt + \sigma_3 z dw_3(t).
\end{aligned} \tag{2.16}$$

Equations (2.15) and (2.16) represent the deterministic and stochastic models respectively where x denotes the size of the sound prey, y denotes the size of the infected prey populations, z represents the predator population, σ denotes the coefficient of the disease transmission factor, δ_1 δ_2 are coefficients of nonlinear prey refuges, h is the constant rate of harvesting of the predator species, σ_i, i = 1, 2, 3 represent the coefficients of the environmental stochastic effects on the sound and infected prey, and predator populations respectively, w_i's i = 1, 2, 3 are standard Brownian motions. From the analysis, gradual increments in both the disease transmission factor and the predator's harvesting rate correspond to a decline in predator population density. This analytical approach aids in understanding the complex interplay of parameters and their effects on the dynamics of the ecosystem. However, the study does not seem to address multi-patch ecosystem dynamics explicitly. In natural ecosystems, species often inhabit multiple interconnected patches, leading to complex migration patterns and local interactions. Ignoring these can oversimplify the model and reduce its ecological realism.

A research was done on the dynamics of a generalist predator–prey system with harvesting and hunting cooperation in deterministic/stochastic environment [1]. The study explored a predator–prey system characterized by generalist predators exhibiting cooperative behavior during hunting, subject to nonlinear harvesting rate. Two models were formulated. First, a mathematical representation for a predator–prey system within an ecological community, assuming a noise-free environment and secondly, a stochastic model to evaluate the impact of randomly fluctuating environments (white noise is introduced into the deterministic system) on the dynamics of the specified predator–prey system. The models for the predator-prey dynamics are;

$$\begin{aligned} \frac{dx}{dt} &= rx(1-\frac{x}{k}) - \beta(1+\alpha y)xy, \\ \frac{dy}{dt} &= \beta\beta_1(1+\alpha y)xy + \frac{\eta y}{1+\eta_0} - d_1 y - d_2 y^2 - \frac{qy}{m_1+m_2 y}. \end{aligned} \tag{2.17}$$

$$
\begin{aligned}
dx &= (rx(1-\frac{x}{k}) - \beta(1+\alpha y)xy)dt + \sigma_1 x(t)dB_1(t), \\
dy &= (\beta\beta_1(1+\alpha y)xy + \frac{\eta y}{1+\eta_0} - d_1 y - d_2 y^2 - \frac{qy}{m_1+m_2 y})dt + \sigma_2 y(t)dB_2(t). \quad (2.18)
\end{aligned}
$$

Equations (2.17) and (2.18) represent the deterministic and stochastic models respectively where x and y represent the densities of prey and predator populations, respectively, at any given time t, β is the consumption rate of prey by predators, β_1 is the conversion efficiency of prey biomass into predator biomass is represented, α is the strength of predator cooperation, η is the reproduction rate of predators, σ_1 and σ_2 correspond to the intensities characterizing the white noises, $B_1(t)$ and $B_2(t)$ represent independent Brownian motions. Analysis showed that increasing the quantity of additional foods for predators might lead to the extinction of prey species while bolstering the abundance of predators. Moreover, despite the ongoing harvesting of predators in the ecosystem, there exists potential for their sustained existence with reduced food resources, provided they engage in cooperative hunting activities. However, the model simplifies the interaction dynamics by focusing on only a single-patch ecosystem. In natural ecosystems, interactions are typically more complex, involving multiple predators, prey, and other environmental factors that can influence outcomes.

2.6 Research Gap and Motivation for the Study

Predator prey models predict a broad range of results based on the nature of interactions between the predators, the prey and the ecosystem. Despite significant advances in the study of predator-prey dynamics, there remain critical gaps in our understanding, particularly when considering stochastic influences, multi-patch ecosystems, and optimal harvesting strategies concurrently. Existing literature predominantly focuses on deterministic models incorporating optimum harvesting policy involving two ecosystems or less. Moreover, while stochastic models have been employed to account for randomness and uncertainty in ecological interactions, these studies

are often limited to single-patch ecosystems. The stochastic dynamics of predator prey models involving more than two ecosystems has been given little attention. Therefore, this research developed a stochastic predator prey model with optimum harvesting for three ecosystems namely "cages" which are within a lake, ensuring that the prey population does not go to extinction. The dynamics of the prey population can transfer from one cage to the other.

CHAPTER THREE

MODEL DEVELOPMENT

3.1 Introduction

In this chapter, we formulate a mathematical model to study predator-prey dynamics with stochastic effects and harvesting. In Section 3.2, we outline the assumptions made in constructing the model. Section 3.3 presents the limitations of the model. In Sections 3.4, 3.5 and 3.6, we describe the model formulation, and define the variables as well as parameters, respectively. Section 3.7 illustrates the model structure using a schematic diagram, while in Section 3.8, we derive the model equations, distinguishing between the deterministic (without noise) and stochastic (with noise) cases.

3.2 Assumptions of the model

The developed model was based on assumptions that;

(i) There is constant migration of fingerlings of the prey between patches.

(ii) Each patch within the ecosystem is homogenous in terms of environmental conditions (water temperature, pH level, as well as water flow and exchange rates of waste products) and resource availability (food supply, water quality).

(iii) Harvesting rates are controlled and can be optimized.

(iv) The fish population is assumed to exhibit stochastic fluctuations that can be modeled as white noise.

(v) Each cage (patch) has different fish population.

(vi) The growth of prey in each patch is assumed to be logistic in the absence of predators.

(vii) Stochasticity in the model arises from the unbounded variation in the population.

3.3 Limitation of the model

The model cannot be generalized. The parameter values, migration structure, and stochastic components are tailored to this three-patch system and may not directly apply to ecosystems with different spatial scales and species compositions.

3.4 Model Formulation

The total fish population under study, denoted by $V(t)$, comprises six interacting classes across three distinct patches: prey population in patch-1 (N_1), predator population in patch-1 (M_1), prey population in patch-2 (N_2), predator population in patch-2 (M_2), prey population in patch-3 (N_3), and predator population in patch-3 (M_3). Each patch is enclosed by mesh structures that allow free movement of fingerlings of the prey species between patches, resulting in interconnected dynamics. The prey in each patch grows logistically with intrinsic growth rate r_i and carrying capacity K_i, while predators feed on prey at a rate a_i, contributing to predator growth at rate γ_i. Both prey and predators are subject to harvesting at rates ν_i, and predators experience natural mortality at rate μ_i. Migration of prey between patches is governed by directional rates α_1 through α_6. Each patch supports a different population size due to spatial heterogeneity. Stochasticity is introduced through white noise terms $\mathrm{d}\eta_t$, $\mathrm{d}\xi_t$, and $\mathrm{d}\varepsilon_t$, capturing unbounded variations in the population over time. The model is described by a system of stochastic differential equations that account for both the deterministic biological interactions and the unbounded variations in the population.

3.5 Variables of the model

Variables used in the model were;

1. N_1(t) - Population of prey species at time t in patch-1.

2. M_1(t) - Population of predators at time t in patch-1.

3. N_2(t) - Population of prey species at time t in patch-2.

4. M_2(t) - Population of predators at time t in patch-2.

5. N_3(t) - Population of prey species at time t in patch-3.

6. M_3(t) - Population of predators at time y in patch-3.

The variables N_1(t), N_2(t), N_3(t), M_1(t), M_2(t) and M_3(t) were used as N_1, N_2, N_3, M_1, M_2, and M_3 respectively for simplicity of the model.

3.6 Parameters of the model

The following table summarises all the parameters used in the model;

Table 3.1: Description of model parameters.

Parameter	Description
ν_i	Harvesting rate in the patches, i =1, 2, 3
K_i	Carrying capacity of prey species in the patches, i =1, 2, 3
a_i	Predation rate in the patches, i =1, 2, 3
r_i	Intrinsic growth rate of prey in the patches, i =1, 2, 3
μ_i	Predator death rate in the patches, i =1, 2, 3
γ_i	Growth rate of predators in the patches, i =1, 2, 3
σ_i	Intensity of stochastic fluctuations, i =1, 2, 3
α_1	Portion of the prey that migrates from patch-1 that get into patch-2
α_2	Portion of the prey that migrates from patch-2 that get into patch-3
α_3	Portion of the prey that migrates from patch-3 that get into patch-1
α_4	Portion of the prey that migrates from patch-2 that get into patch-1
α_5	Portion of the prey that migrates from patch-3 that get into patch-2
α_6	Portion of the prey that migrates from patch-1 that get into patch-3

3.7 Schematic diagram of the Model

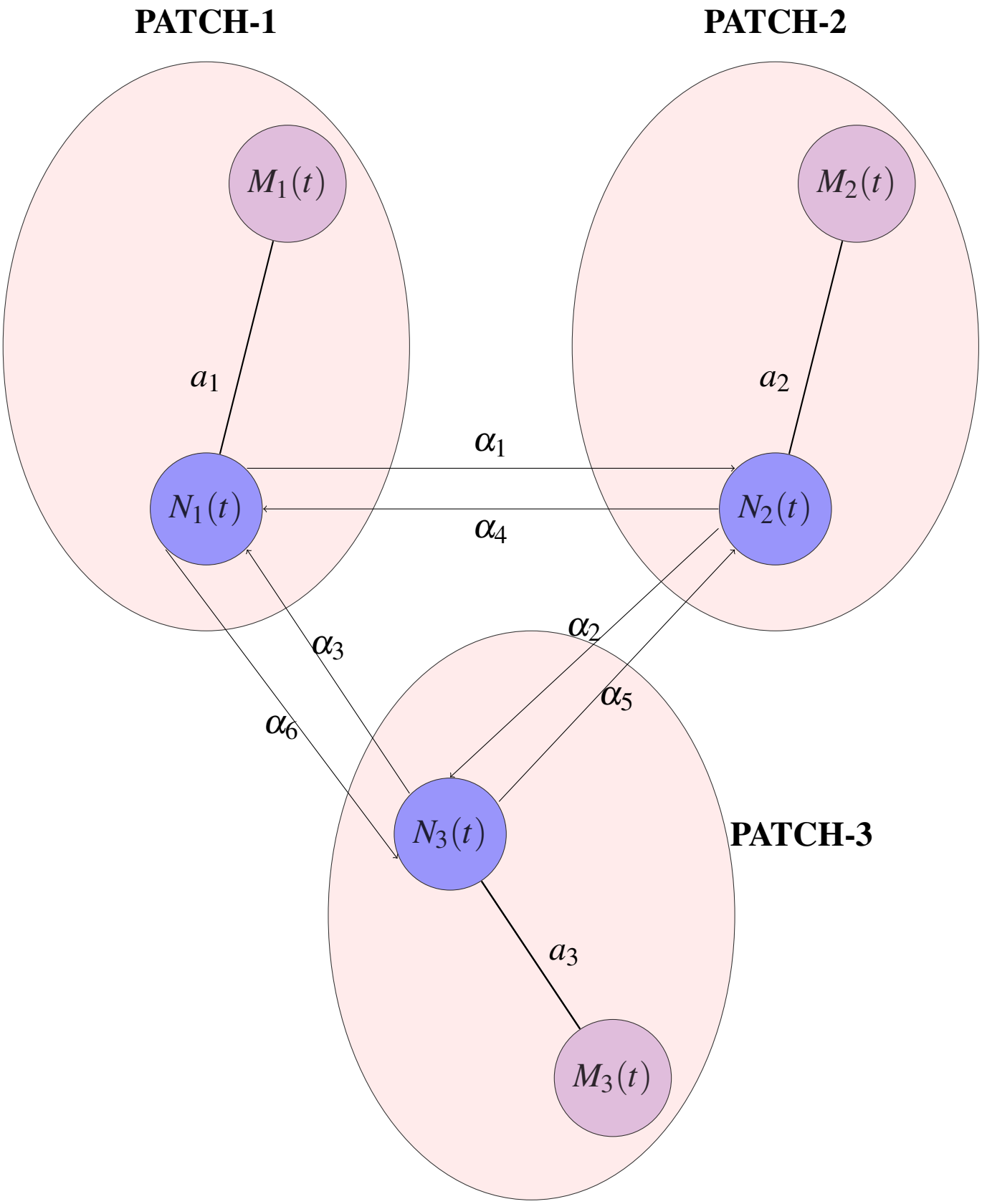

Figure 3.1: Schematic representation of the model.

3.8 The model equations

From the schematic representation, the developed model can be expressed by the following system of equations with respect to time t. Here, $i = 1,2,3$ denotes the three spatially distinct patches. For each patch i, $N_i(t)$ and $M_i(t)$ represent the prey and predator populations, respectively.

3.8.1 Model equations without noise (Deterministic Case)

In this subsection, we present the deterministic form of the model, which governs the population dynamics of prey and predator species across three spatially distinct patches, in the absence of random perturbations.

$$\begin{aligned}
\frac{dN_1}{dt} &= r_1N_1(1-\frac{N_1}{K_1}) - a_1N_1M_1 - \nu_1N_1 + \alpha_4N_2 + \alpha_3N_3 - (\alpha_1+\alpha_6)N_1,\\
\frac{dM_1}{dt} &= \gamma_1N_1M_1 - \mu_1M_1 - \nu_1M_1,\\
\frac{dN_2}{dt} &= r_2N_2(1-\frac{N_2}{K_2}) - a_2N_2M_2 - \nu_2N_2 + \alpha_1N_1 + \alpha_5N_3 - (\alpha_2+\alpha_4)N_2,\\
\frac{dM_2}{dt} &= \gamma_2N_2M_2 - \mu_2M_2 - \nu_2M_2,\\
\frac{dN_3}{dt} &= r_3N_3(1-\frac{N_3}{K_3}) - a_3N_3M_3 - \nu_3N_3 + \alpha_2N_2 + \alpha_6N_1 - (\alpha_3+\alpha_5)N_3,\\
\frac{dM_3}{dt} &= \gamma_3N_3M_3 - \mu_3M_3 - \nu_3M_3. \qquad (3.1)
\end{aligned}$$

where $r_iN_i(1-N_i/K_i)$ is the logistic growth of prey in patch i ($i = 1,2,3$), K_i is the carrying capacity, $a_iN_iM_i$ is the predation rate (reduction in prey due to consumption by predators), ν_iN_i and ν_iM_i are the harvesting rates of prey and predator respectively, α_j is the migration coefficients (proportion of prey moving between patches, $j = 1,2,3,4,5,6$), $\gamma_iN_iM_i$ is the growth of predator population due to predation, and μ_iM_i is the natural mortality rate of predators.

3.8.2 Model equations with noise (Stochastic Case)

This subsection introduces the stochastic extension of the model, in which the unbounded variations in the population are incorporated through white noise terms to account for random disturbances affecting the system dynamics.

$$\begin{aligned}
dN_1 &= (r_1N_1(1-\frac{N_1}{K_1}) - a_1N_1M_1 - \nu_1N_1 + \alpha_4N_2 + \alpha_3N_3 - (\alpha_1+\alpha_6)N_1)dt + \sigma_1N_1d\eta_t,\\
dM_1 &= (\gamma_1N_1M_1 - \mu_1M_1 - \nu_1M_1)dt + \sigma_1M_1d\eta_t,\\
dN_2 &= (r_2N_2(1-\frac{N_2}{K_2}) - a_2N_2M_2 - \nu_2N_2 + \alpha_1N_1 + \alpha_5N_3 - (\alpha_2+\alpha_4)N_2)dt + \sigma_2N_2d\xi_t,\\
dM_2 &= (\gamma_2N_2M_2 - \mu_2M_2 - \nu_2M_2)dt + \sigma_2M_2d\xi_t,\\
dN_3 &= (r_3N_3(1-\frac{N_3}{K_3}) - a_3N_3M_3 - \nu_3N_3 + \alpha_2N_2 + \alpha_6N_1 - (\alpha_3+\alpha_5)N_3)dt + \sigma_3N_3d\varepsilon_t,\\
dM_3 &= (\gamma_3N_3M_3 - \mu_3M_3 - \nu_3M_3)dt + \sigma_3M_3d\varepsilon_t. \qquad (3.2)
\end{aligned}$$

with the initial conditions

$$\begin{aligned}
N_1(0) &= N_1 \geq 0,\\
N_2(0) &= N_2 \geq 0,\\
N_3(0) &= N_3 \geq 0,\\
M_1(0) &= M_1 \geq 0,\\
M_2(0) &= M_2 \geq 0,\\
M_3(0) &= M_3 \geq 0. \qquad (3.3)
\end{aligned}$$

where $d\eta_t = d\xi_t = d\varepsilon_t \sim N(0,dt)$ are the Wiener processes representing the noise, and the total population at time t is given by,

$$V(t) = N_1(t)+N_2(t)+N_3(t)+M_1(t)+M_2(t)+M_3(t) \qquad (3.4)$$

CHAPTER FOUR

STABILITY ANALYSIS OF THE MODEL

4.1 Introduction

In this chapter, we analyze the stability properties of the developed predator-prey model. Section 4.2 addresses the positivity of the model solutions. Section 4.3 examines the boundedness of the model, while Section 4.4 focuses on the existence of equilibrium points, both with and without noise. In Section 4.5, we conduct the stability analysis of the equilibrium points, considering both deterministic and stochastic frameworks.

4.2 Positivity of the model

The variables $N_1, M_1, N_2, M_2, N_3, M_3$ represent populations, so they should remain non-negative.

Lemma 4.2.1. *Under initial conditions (3.3), all the solutions $N_1, M_1, N_2, M_2, N_3, M_3$ of the system (3.1) remain nonnegative for $t \geq 0$*

Proof. For the prey population, the equations for N_1, N_2, N_3 are of the form;

$$\frac{dN_i}{dt} = r_i N_i \left(1 - \frac{N_i}{K_i}\right) - (\text{non-negative terms}) + (\text{migration terms}).$$

The term $r_i N_i \left(1 - \frac{N_i}{K_i}\right)$ is non-negative when $N_i \leq K_i$, $N_i \geq 0$, and $K_i > 0$ as the logistic growth ensures $N_i \geq 0$. Predation $(-a_i N_i M_i)$ and harvesting $(-\nu_i N_i)$, act as sinks but cannot make N_i negative if $N_i \geq 0$. Migration input terms $(\alpha_{ij} N_j)$ are non-negative, adding to the population. Thus, if $N_i(0) \geq 0$, then $\frac{dN_i}{dt}$ ensures $N_i(t) \geq 0$ for all $t \geq 0$.

For the predator population, the equations for M_1, M_2, M_3 are of the form;

$$\frac{dM_i}{dt} = \gamma_i N_i M_i - (\mu_i + \nu_i) M_i.$$

The term $\gamma_i N_i M_i$ is non-negative for $N_i \geq 0$ and $M_i \geq 0$. The mortality terms ($-\mu_i M_i$ and $-\nu_i M_i$) act as sinks but cannot make M_i negative if $M_i \geq 0$. Thus, if $M_i(0) \geq 0$, then $\frac{dM_i}{dt}$ ensures $M_i(t) \geq 0$ for all $t \geq 0$.

The initial conditions $N_i(0) \geq 0$ and $M_i(0) \geq 0$ hold, the structure of the equations ensures that all solutions $N_i(t)$ and $M_i(t)$ remain non-negative for all $t \geq 0$. Thus, positivity of the system. □

4.3 Boundedness of the model

Proposition 4.3.1. *Under initial conditions (3.3), the total population function*

$$V(t) = \sum_{i=1}^{3} (N_i(t) + M_i(t))$$

remains bounded for all $t \geq 0$.

Proof. To prove the boundedness of the solutions for the given system of differential equations, we used the LaSalle Invariance Principle [23] and analyzed the structure of the system. We need to sought a function that is non-negative and has the following properties; decreases along the trajectories of the system, and bounds the populations, meaning it does not increase without bound as $t \to \infty$.

Let the total population of the system be represented by the function;

$$V(t) = N_1(t) + N_2(t) + N_3(t) + M_1(t) + M_2(t) + M_3(t) \tag{4.1}$$

where $N_i(t)$ and $M_i(t)$ denote the prey and predator populations in patch i respectively, for $i = 1, 2, 3$. We aim to show that $V(t)$ remains bounded for all $t \geq 0$. This function was always non-negative because populations cannot be negative.

Differentiating V(t) with respect to time gives;

$$\frac{dV}{dt} = \frac{dN_1}{dt} + \frac{dM_1}{dt} + \frac{dN_2}{dt} + \frac{dM_2}{dt} + \frac{dN_3}{dt} + \frac{dM_3}{dt} \tag{4.2}$$

Substituting the system of equations into this derivative;

$$\begin{aligned}
\frac{dV}{dt} = & \left(r_1 N_1 \left(1 - \frac{N_1}{K_1} \right) - a_1 N_1 M_1 - \nu_1 N_1 + \alpha_4 N_2 + \alpha_3 N_3 - (\alpha_1 + \alpha_6) N_1 \right) \\
& + (\gamma_1 N_1 M_1 - \mu_1 M_1 - \nu_1 M_1) \\
& + \left(r_2 N_2 \left(1 - \frac{N_2}{K_2} \right) - a_2 N_2 M_2 - \nu_2 N_2 + \alpha_1 N_1 + \alpha_5 N_3 - (\alpha_2 + \alpha_4) N_2 \right) \\
& + (\gamma_2 N_2 M_2 - \mu_2 M_2 - \nu_2 M_2) \\
& + \left(r_3 N_3 \left(1 - \frac{N_3}{K_3} \right) - a_3 N_3 M_3 - \nu_3 N_3 + \alpha_2 N_2 + \alpha_6 N_1 - (\alpha_3 + \alpha_5) N_3 \right) \\
& + (\gamma_3 N_3 M_3 - \mu_3 M_3 - \nu_3 M_3)
\end{aligned} \tag{4.3}$$

The right-hand side of the equation (4.3) is a sum of terms that include logistic growth terms which are self-limiting and ensure prey growth does not exceed the carrying capacity K_i, negative interaction terms like $-a_i N_i M_i$, representing predation and reduce prey population when predator numbers increase, mortality and harvesting terms which continuously act to reduce the population sizes, and migration terms which redistribute prey among patches without introducing unbounded growth. The logistic terms inherently bound the prey population by their respective carrying capacities. The mortality and harvesting terms act as sinks, further limiting unbounded growth. Predation introduces nonlinear decay effects, ensuring that even in the presence of high prey numbers, predator pressure helps regulate population sizes. The predator equations similarly contain death and harvesting terms that prevent unbounded growth.

To formalize this, we consider a Lyapunov function,

$$V(t) = \sum_{i=1}^{3} \left(N_i(t) + M_i(t) \right), \tag{4.4}$$

whose derivative satisfy the inequality;

$$\frac{dV}{dt} \leq C - DV(t), \tag{4.5}$$

where $C > 0$ is a constant representing the maximum cumulative contribution from logistic and migration terms, and $D > 0$ is a constant representing the decay effect due to mortality, harvesting, and predation. This inequality implies that $V(t)$ grows at a rate bounded above by a linear function that decreases in V, leading to the conclusion (by the Comparison Theorem [8]) that;

$$V(t) \leq \max\left(V(0), \frac{C}{D}\right), \quad \text{for all } t \geq 0. \tag{4.6}$$

Hence, all individual population components $N_i(t)$ and $M_i(t)$ are bounded above by finite constants. □

4.4 Existence of Equilibrium Points

4.4.1 Equilibrium points without noise

An equilibrium point is a constant solution to a differential equation. To find the equilibrium points of the model without noise, we set the right hand side of the equation to 0. Thus, we have;

$$\begin{aligned}
r_1N_1(1-\frac{N_1}{K_1}) - a_1N_1M_1 - \nu_1N_1 + \alpha_4N_2 + \alpha_3N_3 - (\alpha_1+\alpha_6)N_1 &= 0,\\
\gamma_1N_1M_1 - \mu_1M_1 - \nu_1M_1 &= 0,\\
r_2N_2(1-\frac{N_2}{K_2}) - a_2N_2M_2 - \nu_2N_2 + \alpha_1N_1 + \alpha_5N_3 - (\alpha_2+\alpha_4)N_2 &= 0,\\
\gamma_2N_2M_2 - \mu_2M_2 - \nu_2M_2 &= 0,\\
r_3N_3(1-\frac{N_3}{K_3}) - a_3N_3M_3 - \nu_3N_3 + \alpha_2N_2 + \alpha_6N_1 - (\alpha_3+\alpha_5)N_3 &= 0,\\
\gamma_3N_3M_3 - \mu_3M_3 - \nu_3M_3 &= 0.
\end{aligned} \tag{4.7}$$

The system has at least 3 possible positive equilibria;

1. $E_0(0,0,0,0,0,0)$
2. $E_1(N_1,0,N_2,0,N_3,0)$
3. $E_2(N_1,M_1,N_2,M_2,N_3,M_3)$

We now show the existence of the equilibria as follows;

(i) $E_0(0,0,0,0,0,0)$. The existence of this equilibrium point is trivial, where all species go to extinction.

(ii) $E_1(N_1,0,N_2,0,N_3)$ with $N_1,N_2,N_3 > 0$

Let $M_1,M_2,M_3 = 0$, system (4.7) simplifies to;

$$\begin{aligned} r_1N_1(1-\frac{N_1}{K_1}) - \nu_1N_1 + \alpha_4N_2 + \alpha_3N_3 - (\alpha_1+\alpha_6)N_1 &= 0, \\ r_2N_2(1-\frac{N_2}{K_2}) - \nu_2N_2 + \alpha_1N_1 + \alpha_5N_3 - (\alpha_2+\alpha_4)N_2 &= 0, \\ r_3N_3(1-\frac{N_3}{K_3}) - \nu_3N_3 + \alpha_2N_2 + \alpha_6N_1 - (\alpha_3+\alpha_5)N_3 &= 0. \end{aligned} \tag{4.8}$$

From the last line of equation (4.8);

$$-r_3\frac{N_3^2}{K_3} + (r_3 - \nu_3 - \alpha_3 - \alpha_5)N_3 = -\alpha_2N_2 - \alpha_6N_1$$

Multiplying by -1 and K_3 all through we have;

$$r_3N_3^2 - K_3(r_3 - \nu_3 - \alpha_3 - \alpha_5)N_3 - K_3(\alpha_2N_2 + \alpha_6N_1) = 0$$

Solving by use of the quadratic formula, we have that;

$$N_3^* = \frac{K_3(r_3 - \nu_3 - \alpha_3 - \alpha_5) \pm \sqrt{(K_3(r_3 - \nu_3 - \alpha_3 - \alpha_5))^2 + 4r_3K_3(\alpha_2N_2 + \alpha_6N_1)}}{2r_3} \quad (4.9)$$

Similarly, it can be illustrated that;

$$N_2^* = \frac{K_2(r_2 - \nu_2 - \alpha_2 - \alpha_4) \pm \sqrt{(K_2(r_2 - \nu_2 - \alpha_2 - \alpha_4))^2 + 4r_2K_2(\alpha_1N_1 + \alpha_5N_3)}}{2r_2} \quad (4.10)$$

and

$$N_1^* = \frac{K_1(r_1 - \nu_1 - \alpha_1 - \alpha_6) \pm \sqrt{(K_1(r_1 - \nu_1 - \alpha_1 - \alpha_6))^2 + 4r_1K_1(\alpha_4N_2 + \alpha_3N_3)}}{2r_1} \quad (4.11)$$

Therefore, our equilibrium point is given by $E_1(N_1^*, 0, N_2^*, 0, N_3^*, 0)$.

(iii) $E_2(N_1, M_1, N_2, M_2, N_3, M_3)$ with $N_1, M_1, N_2, M_2, N_3, M_3 > 0$. This is the co-existence equilibrium point.

Equating the right hand side of system (4.7) to 0, we have that;

$$\gamma_3N_3M_3 - \mu_3M_3 - \nu_3M_3 = 0$$

$$M_3(\gamma_3N_3 - \mu_3 - \nu_3) = 0$$

$$\gamma_3N_3 - \mu_3 - \nu_3 = 0$$

$$\gamma_3N_3 = \mu_3 + \nu_3$$

$$N_3^* = \frac{\mu_3 + \nu_3}{\gamma_3}$$

Similarly;

$$N_2^* = \frac{\mu_2 + \nu_2}{\gamma_2}$$

and

$$N_1^* = \frac{\mu_1 + \nu_1}{\gamma_1}$$

$$r_1 N_1 (1 - \frac{N_1}{K_1}) - a_1 N_1 M_1 - \nu_1 N_1 + \alpha_4 N_2 + \alpha_3 N_3 - (\alpha_1 + \alpha_6) N_1 = 0$$

$$r_1 N_1 - \frac{r_1 N_1^2}{K_1} - a_1 N_1 M_1 - \nu_1 N_1 + \alpha_4 N_2 + \alpha_3 N_3 - \alpha_1 N_1 - \alpha_6 N_1 = 0$$

$$r_1 N_1 - \frac{r_1 N_1^2}{K_1} - \nu_1 N_1 + \alpha_4 N_2 + \alpha_3 N_3 - \alpha_1 N_1 - \alpha_6 N_1 = a_1 N_1 M_1$$

$$N_1 (r_1 - \frac{r_1 N_1}{K_1} - \nu_1 - \alpha_1 - \alpha_6 + \frac{\alpha_4 N_2}{N_1} + \frac{\alpha_3 N_3}{N_1}) = N_1 (a_1 M_1)$$

N_1 cancels out and we have;

$$r_1 - \frac{r_1 N_1^*}{K_1} - \nu_1 - \alpha_1 - \alpha_6 + \frac{\alpha_4 N_2^*}{N_1^*} + \frac{\alpha_3 N_3^*}{N_1^*}) = a_1 M_1$$

Replacing the values of N_1^*, N_2^* and N_3^* and making M_1 the subject, we have;

$$M_1^* = \frac{1}{a_1} [r_1 - \frac{r_1 (\mu_1 + \nu_1)^*}{K_1 \gamma_1} - \nu_1 - \alpha_1 - \alpha_6 + \frac{\alpha_4 (\mu_2 + \nu_2) \gamma_1}{\gamma_2 (\mu_1 + \nu_1)} + \frac{\alpha_3 (\mu_3 + \nu_3) \gamma_1}{\gamma_3 (\mu_1 + \nu_1)}] \quad (4.12)$$

Similarly;

$$M_2^* = \frac{1}{a_2}[r_2 - \frac{r_2(\mu_2+\nu_2)^*}{K_2\gamma_2} - \nu_2 - \alpha_2 - \alpha_4 + \frac{\alpha_1(\mu_1+\nu_1)\gamma_2}{\gamma_1(\mu_2+\nu_2)} + \frac{\alpha_5(\mu_3+\nu_3)\gamma_2}{\gamma_3(\mu_2+\nu_2)}] \quad (4.13)$$

and

$$M_3^* = \frac{1}{a_3}[r_3 - \frac{r_3(\mu_3+\nu_3)^*}{K_3\gamma_3} - \nu_3 - \alpha_3 - \alpha_5 + \frac{\alpha_2(\mu_2+\nu_2)\gamma_3}{\gamma_2(\mu_3+\nu_3)} + \frac{\alpha_6(\mu_1+\nu_1)\gamma_3}{\gamma_1(\mu_3+\nu_3)}] \quad (4.14)$$

Therefore, our equilibrium point is given by $E_2(N_1^*, M_1^*, N_2^*, M_2^*, N_3^*, M_3^*)$.

4.5 Stability analysis of the model

4.5.1 Stability analysis without noise

The stability of the system is obtained by computing the Jacobian matrix and obtaining the eigenvalues at each of the equilibrium points. The Jacobian of the system (3.1) is given by;

$$J = \begin{bmatrix} a & \alpha_4 & \alpha_3 & -a_1N_1 & 0 & 0 \\ \gamma_1M_1 & 0 & 0 & \gamma_1N_1 - \mu_1 - \nu_1 & 0 & 0 \\ \alpha_1 & b & 0 & \alpha_5 & -a_2N_2 & 0 \\ 0 & \gamma_2M_2 & 0 & 0 & \gamma_2N_2 - \mu_2 - \nu_2 & 0 \\ \alpha_6 & \alpha_2 & c & 0 & 0 & -a_3N_3 \\ 0 & 0 & \gamma_3M_3 & 0 & 0 & \gamma_3N_3 - \mu_3 - \nu_3 \end{bmatrix}$$

where;

$$\begin{aligned} a &= r_1(1 - \frac{2N_1}{K_1}) - \alpha_1M_1 - \nu_1 - (\alpha_1 + \alpha_6) \\ b &= r_2(1 - \frac{2N_2}{K_2}) - \alpha_2M_2 - \nu_2 - (\alpha_2 + \alpha_4) \\ c &= r_3(1 - \frac{2N_3}{K_3}) - \alpha_3M_3 - \nu_3 - (\alpha_3 + \alpha_5) \end{aligned}$$

The analysis of the stability at each of the equilibrium points is as follows;

(i) $E_0(0,0,0,0,0,0)$. Computing the Jacobian matrix at this equilibrium point yields;

$$J_{E_0} = \begin{bmatrix} -\nu_1 - (\alpha_1 + \alpha_6) & \alpha_4 & \alpha_3 & 0 & 0 & 0 \\ 0 & 0 & 0 & -\mu_1 - \nu_1 & 0 & 0 \\ \alpha_1 & -\nu_2 - (\alpha_2 + \alpha_4) & 0 & \alpha_5 & 0 & 0 \\ 0 & 0 & 0 & 0 & -\mu_2 - \nu_2 & 0 \\ \alpha_6 & \alpha_2 & -\nu_3 - (\alpha_3 + \alpha_5) & 0 & 0 & 0 \\ 0 & 0 & 0 & 0 & 0 & -\mu_3 - \nu_3 \end{bmatrix}$$

The Jacobian matrix at the trivial equilibrium point, J_{E_0}, was formed symbolically but evaluated numerically using MATLAB software. Eigenvalues were computed with MATLAB's built-in *eig* function [$eig(J)$], which returns all the eigen values of the evaluated Jacobian matrix. The output yields an eigen vector D which is a diagonal matrix and contains all the eigen values of the matrix.

$$D = \begin{bmatrix} \lambda_1 & 0 & 0 & 0 & 0 & 0 \\ 0 & \lambda_2 & 0 & 0 & 0 & 0 \\ 0 & 0 & \lambda_3 & 0 & 0 & 0 \\ 0 & 0 & 0 & \lambda_4 & 0 & 0 \\ 0 & 0 & 0 & 0 & \lambda_5 & 0 \\ 0 & 0 & 0 & 0 & 0 & \lambda_6 \end{bmatrix}$$

$$D = \begin{bmatrix} -\mu_1 - \nu_1 & 0 & 0 & 0 & 0 & 0 \\ 0 & -\mu_2 - \nu_2 & 0 & 0 & 0 & 0 \\ 0 & 0 & -\mu_3 - \nu_3 & 0 & 0 & 0 \\ 0 & 0 & 0 & -\alpha_3 - \alpha_5 - \nu_3 & 0 & 0 \\ 0 & 0 & 0 & 0 & d & 0 \\ 0 & 0 & 0 & 0 & 0 & e \end{bmatrix}$$

where;

$$d = -\frac{\alpha_1+\alpha_2+\alpha_4+\alpha_6+\nu_1+\nu_2}{2} - \frac{1}{2}\sqrt{\alpha_1^2-2\alpha_1\alpha_2-2\alpha_1\alpha_4+2\alpha_1\alpha_6+2\alpha_1\nu_1-2\alpha_1\nu_2+4\alpha_3\alpha_1+\alpha_2^2+2\alpha_2\alpha_4-2\alpha_2\alpha_6-2\alpha_2\nu_1+f}$$

$$e = \frac{1}{2}\sqrt{\alpha_1^2-2\alpha_1\alpha_2-2\alpha_1\alpha_4+2\alpha_1\alpha_6+2\alpha_1\nu_1-2\alpha_1\nu_2+4\alpha_3\alpha_1+g} - \frac{\alpha_2+\alpha_4+\alpha_6+\nu_1+\nu_2+\alpha_1}{2}$$

and that the f and g in d and e equation represents;

$$f = 2\alpha_2\nu_2+\alpha_4^2-2\alpha_4\alpha_6-2\alpha_4\nu_1+2\alpha_4\nu_2+\alpha_6^2+2\alpha_6\nu_1-2\alpha_6\nu_2+\nu_1^2-2\nu_1\nu_2+\nu_2^2$$

$$g = \alpha_2^2+2\alpha_2\alpha_4-2\alpha_2\alpha_6-2\alpha_2\nu_1+2\alpha_2\nu_2+\alpha_4^2-2\alpha_4\alpha_6-2\alpha_4\nu_1+2\alpha_4\nu_2+\alpha_6^2+2\alpha_6\nu_1-2\alpha_6\nu_2+\nu_1^2-2\nu_1\nu_2+\nu_2^2$$

$$\begin{aligned}
\lambda_1 &= -(\mu_1+\nu_1),\\
\lambda_2 &= -(\mu_2+\nu_2),\\
\lambda_3 &= -(\mu_3+\nu_3),\\
\lambda_4 &= -(\alpha_3+\alpha_5+\nu_3),\\
\lambda_5 &= d,\\
\lambda_6 &= e.
\end{aligned}$$

The first four eigenvalues, $\lambda_{1,2,3,4}$ are negative. The remaining two eigenvalues, λ_5 and λ_6, arise from the 2×2 sub-block of the Jacobian matrix and are obtained from its characteristic equation;

$$\lambda^2 - T\lambda + \Delta = 0,$$

where $T = \mathrm{tr}(J_p)$ is the trace and $\Delta = \det(J_p)$ is the determinant of the 2×2 submatrix J_p. The eigenvalues are therefore given by

$$\lambda_{5,6} = \frac{T \pm \sqrt{T^2-4\Delta}}{2}.$$

If $\Delta < 0$, the eigenvalues are real and of opposite signs. If $\Delta > 0$ and $T < 0$, both eigenvalues are negative, if $\Delta > 0$ and $T > 0$, both are positive. If $T^2 - 4\Delta < 0$, the eigenvalues are complex with real part $T/2$, and their stability depends on the sign of T.

The Δ of the 2 $\times$ 2 sub-block is negative (d $\times$ e - 0, d has a negative sign and e is positive), implying that one eigenvalue (λ_5) is positive and the other (λ_6) is negative. Therefore, the trivial equilibrium point E_0 has five negative and one positive eigenvalues. This implies that it is a saddle point and hence unstable. This implies that the predator-prey ecosystem is prone to instability, where small disturbances could lead to significant shifts in population dynamics, potentially resulting in species extinction or exponential growth of population.

(ii) $E_1(N_1^*, 0, N_2^*, 0, N_3^*, 0)$. Computing the Jacobian matrix at this equilibrium point yields;

$$J_{E_1} = \begin{bmatrix} h & \alpha_4 & \alpha_3 & -a_1 N_1^* & 0 & 0 \\ 0 & 0 & 0 & \gamma_1 N_1^* - \mu_1 - \nu_1 & 0 & 0 \\ \alpha_1 & r_2(1 - \frac{2N_2^*}{K_2}) - \nu_2 - (\alpha_2 + \alpha_4) & 0 & \alpha_5 & -a_2 N_2^* & 0 \\ 0 & 0 & 0 & 0 & \gamma_2 N_2^* - \mu_2 - \nu_2 & 0 \\ \alpha_6 & \alpha_2 & r_3(1 - \frac{2N_3^*}{K_3}) - \nu_3 - (\alpha_3 + \alpha_5) & 0 & 0 & -a_3 N_3^* \\ 0 & 0 & 0 & 0 & 0 & \gamma_3 N_3^* - \mu_3 - \nu_3 \end{bmatrix}$$

where;

$$h = r_1(1 - \frac{2N_1^*}{K_1}) - \nu_1 - (\alpha_1 + \alpha_6)$$

The determinant of J_{E_1} with the help of MATLAB software is;

$$
\begin{aligned}
&(\mu_1+\nu_1-N_1^*\gamma_1)(\mu_2+\nu_2-N_2^*\gamma_2)(\mu_3+\nu_3-N_3^*\gamma_3)\\
&\qquad\times\Big(K_2K_3\alpha_1\alpha_2\alpha_3+K_2K_3\alpha_1\alpha_3\alpha_4+K_2K_3\alpha_1\alpha_4\alpha_5+K_2K_3\alpha_2\alpha_3\alpha_6+K_2K_3\alpha_3\alpha_4\alpha_6\\
&\quad+K_2K_3\alpha_2\alpha_3h+K_2K_3\alpha_2\alpha_5h+K_2K_3\alpha_3\alpha_4h+K_2K_3\alpha_4\alpha_5h+K_2K_3\alpha_1\alpha_4\nu_3+K_2K_3\alpha_3\alpha_6\nu_2\\
&\quad-K_2K_3\alpha_1\alpha_4r_3-K_2K_3\alpha_3\alpha_6r_2+2K_2N_3^*\alpha_1\alpha_4r_3+2K_3N_2^*\alpha_3\alpha_6r_2+K_2K_3\alpha_2h\nu_3+K_2K_3\alpha_3h\nu_2\\
&\quad+K_2K_3\alpha_4h\nu_3+K_2K_3\alpha_5h\nu_2-K_2K_3\alpha_2hr_3-K_2K_3\alpha_3hr_2-K_2K_3\alpha_4hr_3-K_2K_3\alpha_5hr_2\\
&\quad+2K_2N_3^*\alpha_2hr_3+2K_3N_2^*\alpha_3hr_2+2K_2N_3^*\alpha_4hr_3+2K_3N_2^*\alpha_5hr_2+K_2K_3h\nu_2\nu_3-K_2K_3h\nu_2r_3\\
&\quad-K_2K_3h\nu_3r_2+2K_2N_3^*h\nu_2r_3+2K_3N_2^*h\nu_3r_2+K_2K_3hr_2r_3-2K_2N_3^*hr_2r_3-2K_3N_2^*hr_2r_3\\
&\qquad\qquad+4N_2^*N_3^*hr_2r_3\Big)
\end{aligned}
\tag{4.15}
$$

Let

$$P \;=\; \prod_{i=1}^{3}\left(\mu_i+\nu_i-N_i^*\gamma_i\right) \quad \text{and} \quad B \;=\; \Big(\text{big bracket expression in equation (4.15)}\Big).$$

Then,

$$\det(J_{E_1}) \;=\; P\cdot B.$$

The $\det(J_{E_1})>0$ if and only if either $P>0$ and $B>0$, or $P<0$ and $B<0$. P is the product of three factors, $P>0$ when an even number of the factors $\mu_i+\nu_i-N_i^*\gamma_i$ are negative (i.e. 0 or 2 negatives), and $P<0$ when an odd number are negative (1 or 3 negatives).

If each term $\mu_i+\nu_i-N_i^*\gamma_i>0$ and $B>0$ hold then,

$$\det(J_{E_1})>0$$

The trace of J_{E_1} is given by;

$$\begin{aligned} \mathrm{Tr}(J_{E_1}) &= r_1\left(1-\frac{2N_1^*}{K_1}\right)-\nu_1-(\alpha_1+\alpha_6) \\ &\quad +\gamma_3 N_3^*-\mu_3-\nu_3 \end{aligned} \tag{4.16}$$

Since $r_1\left(1-\frac{2N_1^*}{K_1}\right)$ and $\gamma_3 N_3^*$ are bounded growth terms, while the remaining terms $-(\mu_3+\nu_3)-\nu_1-(\alpha_1+\alpha_6)$ are strictly negative by definition, their combined effect dominates the positive contributions. Consequently, the overall trace of J_{E_1} remains negative, i.e.,

$$\mathrm{Tr}(J_{E_1})<0.$$

Since $\mathrm{Tr}(J_{E_1})<0$ and $\det(J_{E_1})>0$, the equilibrium point E_1 is locally asymptotically stable. This implies a balanced ecosystem where predator and prey populations can coexist stably, with oscillations around the equilibrium point.

(iii) $E_2(N_1^*,M_1^*,N_2^*,M_2^*,N_3^*,M_3^*)$. Computing the Jacobian matrix at this equilibrium point yields;

$$J_{E_2}=\begin{bmatrix} s & \alpha_4 & \alpha_3 & -a_1\frac{\mu_1+\nu_1}{\gamma_1} & 0 & 0 \\ \gamma_1 M_1^* & 0 & 0 & 0 & 0 & 0 \\ \alpha_1 & t & 0 & \alpha_5 & -a_2\frac{\mu_2+\nu_2}{\gamma_2} & 0 \\ 0 & \gamma_2 M_2^* & 0 & 0 & 0 & 0 \\ \alpha_6 & \alpha_2 & u & 0 & 0 & -a_3\frac{\mu_3+\nu_3}{\gamma_3} \\ 0 & 0 & \gamma_3 M_3^* & 0 & 0 & 0 \end{bmatrix}$$

where;

$$
\begin{aligned}
s &= r_1\left(1-\frac{2(\mu_1+\nu_1)}{K_1\gamma_1}\right)-\alpha_1 M_1^*-\nu_1-(\alpha_1+\alpha_6)\\
t &= r_2\left(1-\frac{2(\mu_2+\nu_2)}{K_2\gamma_2}\right)-\alpha_2 M_2^*-\nu_2-(\alpha_2+\alpha_4)\\
u &= r_3\left(1-\frac{2(\mu_3+\nu_3)}{K_3\gamma_3}\right)-\alpha_3 M_3^*-\nu_3-(\alpha_3+\alpha_5)
\end{aligned}
$$

The trace of J_{E_2} is given by;

$$
\mathrm{Tr}(J_{E_2}) = s+0+0+0+0+0
$$

$$
\mathrm{Tr}(J_{E_2}) = \left(r_1\left(1-\frac{2(\mu_1+\nu_1)}{K_1\gamma_1}\right)-\alpha_1 M_1^*-\nu_1-(\alpha_1+\alpha_6)\right) \tag{4.17}
$$

The determinant of J_{E_2} with the help of MATLAB software is;

$$
-M_1^* M_2^* M_3^* a_1 a_2 a_3(\mu_1+\nu_1)(\mu_2+\nu_2)(\mu_3+\nu_3) \tag{4.18}
$$

From definition, $a_i < 0$ and $(\mu_i+\nu_i) < 0$ for $i = 1,2,3$, while $M_i^* > 0$, the product $a_1a_2a_3(\mu_1+\nu_1)(\mu_2+\nu_2)(\mu_3+\nu_3)$ is positive. Consequently, the leading negative sign ensures that;

$$
\det(J_{E2}) < 0
$$

The negative determinant already implies instability. The equilibrium point is unstable and this implies that minor disturbances can lead to the extinction of species or exponential growth of

population.

4.5.2 Stability analysis with noise

$$
\begin{aligned}
dN_1 &= (r_1N_1(1-\frac{N_1}{K_1}) - a_1N_1M_1 - \nu_1N_1 + \alpha_4N_2 + \alpha_3N_3 - (\alpha_1+\alpha_6)N_1)dt + \sigma_1N_1d\eta_t,\\
dM_1 &= (\gamma_1N_1M_1 - \mu_1M_1 - \nu_1M_1)dt + \sigma_1M_1d\eta_t,\\
dN_2 &= (r_2N_2(1-\frac{N_2}{K_2}) - a_2N_2M_2 - \nu_2N_2 + \alpha_1N_1 + \alpha_5N_3 - (\alpha_2+\alpha_4)N_2)dt + \sigma_2N_2d\xi_t,\\
dM_2 &= (\gamma_2N_2M_2 - \mu_2M_2 - \nu_2M_2)dt + \sigma_2M_2d\xi_t,\\
dN_3 &= (r_3N_3(1-\frac{N_3}{K_3}) - a_3N_3M_3 - \nu_3N_3 + \alpha_2N_2 + \alpha_6N_1 - (\alpha_3+\alpha_5)N_3)dt + \sigma_3N_3d\varepsilon_t,\\
dM_3 &= (\gamma_3N_3M_3 - \mu_3M_3 - \nu_3M_3)dt + \sigma_3M_3d\varepsilon_t. \qquad (4.19)
\end{aligned}
$$

A standard Stochastic Differential Equations (SDEs) takes the form;

$$dx_i = f_i(x)dt + g_i(x)dW_i(t), \quad i = 1,2,3,...,n \qquad (4.20)$$

where $f_i(x)$ captures deterministic dynamics, $g_i(x)$ incorporates stochastic effects, and $W_i(t)$ are Wiener processes representing the random fluctuations (Brownian Motion).

We can rewrite (4.19) in a general form as;

$$
\begin{aligned}
dN_i &= f_i(N,M)\,dt + g_i(N,M)\,dW_i(t), \quad i = 1,2,3\\
dM_i &= h_i(N,M)\,dt + k_i(N,M)\,dW_i(t). \quad i = 1,2,3 \qquad (4.21)
\end{aligned}
$$

where $f_i(N,M)$ is the deterministic component of N_i, $g_i(N,M)$ is the stochastic component of N_i, $h_i(N,M)$ is the deterministic component of M_i, $k_i(N,M)$ is the stochastic component of M_i, and $dW_i(t)$ represent the Wiener processes.

We define the Lyapunov function as;

$$V(N,M) = \sum_{i=1}^{3}\left(\frac{N_i^2}{2}+\frac{M_i^2}{2}\right). \tag{4.22}$$

which measures the "energy" or total population in the system.

Computing the partial derivatives of $V(N,M)$, we have;

$$\begin{aligned}
\frac{\partial V}{\partial N_i} &= N_i,\\
\frac{\partial V}{\partial M_i} &= M_i,\\
\frac{\partial^2 V}{\partial N_i^2} &= 1,\\
\frac{\partial^2 V}{\partial M_i^2} &= 1.
\end{aligned} \tag{4.23}$$

For i = 1, equation (4.21) yields;

$$\begin{aligned}
dN_1 &= f_1(N,M)\,dt + g_1(N,M)\,dW_1,\\
dM_1 &= h_1(N,M)\,dt + k_1(N,M)\,dW_1.
\end{aligned} \tag{4.24}$$

where;

$$\begin{aligned}
f_1(N,M) &= r_1N_1\left(1-\frac{N_1}{K_1}\right) - a_1N_1M_1 - \nu_1N_1 + \alpha_4N_2 - (\alpha_1+\alpha_6)N_1,\\
g_1(N,M) &= \sigma_1N_1,\\
h_1(N,M) &= \gamma_1N_1M_1 - \mu_1M_1 - \nu_1M_1,\\
k_1(N,M) &= \sigma_1M_1.
\end{aligned}$$

Applying the Itô's Lemma [15], the stochastic differential of $V(N,M)$ becomes;

$$dV = \sum_{i=1}^{3}\left(\frac{\partial V}{\partial N_i}dN_i + \frac{\partial V}{\partial M_i}dM_i\right) + \frac{1}{2}\sum_{i=1}^{3}\left(\frac{\partial^2 V}{\partial N_i^2}(dN_i)^2 + \frac{\partial^2 V}{\partial M_i^2}(dM_i)^2\right). \quad (4.25)$$

Substituting equations (4.23) and (4.24) in equation (4.25), we have;

$$dV = \sum_{i=1}^{3}\left(N_i f_i + M_i h_i\right)dt + \sum_{i=1}^{3}\left(N_i g_i + M_i k_i\right)dW_i + \frac{1}{2}\sum_{i=1}^{3}\left(g_i^2 + k_i^2\right)dt. \quad (4.26)$$

where, $N_i f_i$ and $M_i h_i$ contribute to the deterministic drift term, $N_i g_i$ and $M_i k_i$ are associated with the stochastic terms, $g_i^2 + k_i^2$ contribute to the second-order term.

The deterministic term in dV becomes;

$$\begin{aligned} N_1 f_1 + M_1 h_1 &= N_1\left[r_1 N_1\left(1 - \frac{N_1}{K_1}\right) - a_1 N_1 M_1 - \nu_1 N_1 + \alpha_4 N_2 - (\alpha_1 + \alpha_6)N_1\right] \\ &\quad + M_1\left[\gamma_1 N_1 M_1 - \mu_1 M_1 - \nu_1 M_1\right]. \end{aligned} \quad (4.27)$$

The stochastic term in dV becomes;

$$N_1 g_1 + M_1 k_1 = N_1(\sigma_1 N_1) + M_1(\sigma_1 M_1). \quad (4.28)$$

The second-order term in dV becomes;

$$g_1^2 + k_1^2 = (\sigma_1 N_1)^2 + (\sigma_1 M_1)^2. \quad (4.29)$$

Therefore, the full equation for $i = 1$ is;

$$
\begin{aligned}
dV_1 &= \left(r_1 N_1^2 - \frac{r_1 N_1^3}{K_1} - a_1 N_1^2 M_1 - \nu_1 N_1^2 + \alpha_4 N_1 N_2 - (\alpha_1 + \alpha_6) N_1^2 + \gamma_1 N_1 M_1^2 - \mu_1 M_1^2 - \nu_1 M_1^2\right) dt \\
&\quad + \left(\sigma_1 N_1^2 + \sigma_1 M_1^2\right) dW_1 + \frac{1}{2}\left(\sigma_1^2 N_1^2 + \sigma_1^2 M_1^2\right) dt
\end{aligned} \tag{4.30}
$$

For $i = 2$ and $i = 3$, with corresponding terms for f_2, h_2, g_2, k_2 and f_3, h_3, g_3, k_3, the general form can be represented as;

$$
dV = \sum_{i=1}^{3} \left[(N_i f_i + M_i h_i)\, dt + (N_i g_i + M_i k_i)\, dW_i + \frac{1}{2}\left(g_i^2 + k_i^2\right) dt \right] \tag{4.31}
$$

To ensure stochastic stability, the expected change in the Lyapunov function, $V(N, M)$, should be decreasing. That is,

$$
\mathbb{E}\left[\frac{dV}{dt}\right] = \sum_{i=1}^{3} \left[N_i f_i + M_i h_i + \frac{1}{2}(g_i^2 + k_i^2) \right] < 0. \tag{4.32}
$$

This is achieved when; drift terms dominate and are negative, harvesting rates ν_i and mortality rates μ_i are large enough, noise intensities σ_i are not too large, and predator efficiency γ_i and prey growth r_i are not excessively high.

Numerical results

Following the analytic derivation of the Lyapunov function and the conditions for stochastic stability, we now present numerical simulations done using the Euler-Maruyama method [2] to illustrate the system's behavior under different parameter regimes.

The Lyapunov function, V(t) was computed at each time step as;

$$
V(t) = \sum_{i=1}^{3} \frac{N_i(t)^2 + M_i(t)^2}{2}
$$

To ensure stochastic stability, we need to show that $V(t)$ remains bounded (decreases in expectation). Lyapunov Function,

$$LV < 0 \Rightarrow (e_i - 1) < 0 \Rightarrow e_i < 1 \tag{4.33}$$

$LV < 0$ ensures mean squared stability, and it decays over time. For this to hold, e_i (predator's efficiency in converting prey into a new predator) must satisfy $e_i < 1$. Not all prey consumed translates to predator growth, some energy is lost through metabolic processes. Ecologically, the system achieves sustainable balance which allows co-existence of species. Ultimately, this prevents extinction of species and promotes long term ecological stability.

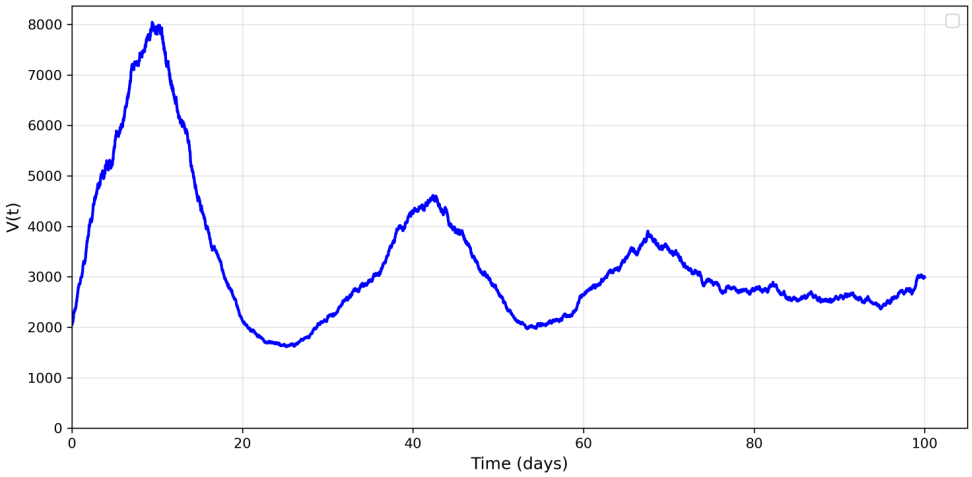

Figure 4.1: Lyapunov Function V(t) over Time when $e_i < 1$.

In Figure 4.1, when $e_i < 1$, $V(t)$ stays bounded (decreases over time) indicating stochastic stability. This implies that the model is resilient to environmental noise and the populations tend to stabilize despite randomness.

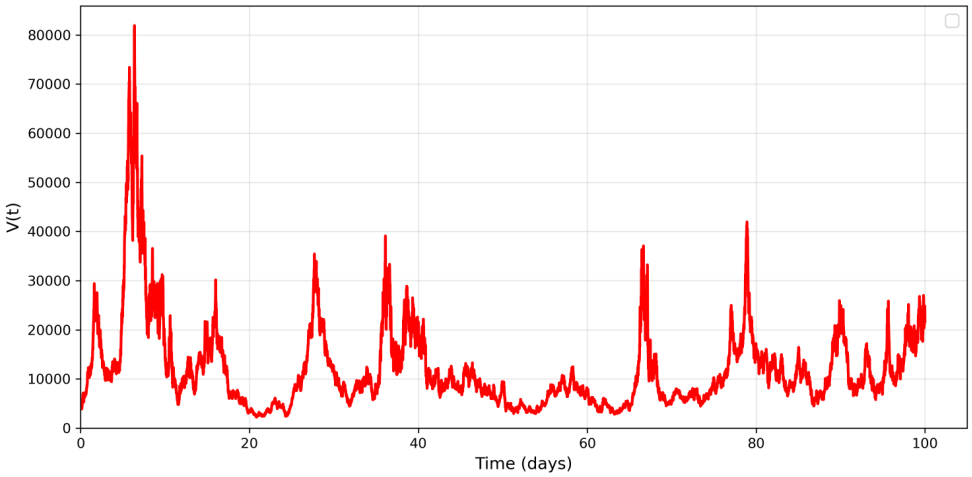

Figure 4.2: Lyapunov Function V(t) over Time when $e_i > 1$.

In Figure 4.2, when $e_i > 1$, $V(t)$ grows without bound (drifts upward indefinitely) indicating that the system is unstable. This suggests that the lack of harvesting or high intensity of noise disrupts the system that highlights the significance of harvesting and mortality processes in regulating ecological balance particularly when there is uncertainty in the environment.

CHAPTER FIVE

OPTIMAL CONTROL OF HARVESTING

5.1 Introduction

In managing biological resources, one of the critical challenges is determining how to harvest populations sustainably while maintaining ecological stability. In this chapter, we formulate and analyze an optimal control problem where prey is subject to harvesting in the presence of predators. Section 5.2 presents the formulation of the controlled predator-prey model, incorporating harvesting effort as a control variable. In Section 5.3, we define the objective functional that aims to balance economic returns from harvesting with the cost of effort. Sections 5.4 and 5.5 apply Pontryagin's Maximum Principle to derive the necessary conditions for optimality, including the Hamiltonian, adjoint equations, and the expression for the optimal control. The outcomes of these optimal strategies are further analyzed using numerical simulations, demonstrating the benefits of adaptive harvesting over fixed-rate approaches.

5.2 Controlled Model Formulation

Let $x_i(t)$ and $y_i(t)$ denote the prey and predator populations in patch i $(i = 1,2,3)$ at time t. The system of nonlinear ordinary differential equations is given by;

$$\begin{aligned} \frac{dx_i}{dt} &= r_i x_i \left(1 - \frac{x_i}{K_i}\right) - a_i x_i y_i - u_i(t) x_i, \\ \frac{dy_i}{dt} &= b_i x_i y_i - d_i y_i, \end{aligned} \tag{5.1}$$

where, r_i is the intrinsic growth rate of the prey, K_i is the carrying capacity of the prey, a_i is the predation rate, b_i is the conversion efficiency of prey to predator biomass, d_i is the natural death rate of the predator, and $u_i(t)$ is the control function representing harvesting effort.

The control variable $u_i(t)$ is bounded within realistic management limits;

$$0 \leq u_i(t) \leq u_{\max}, \tag{5.2}$$

where $u_{\max}$ is the maximum allowable harvesting effort beyond which overexploitation would occur.

The harvesting term $u_i(t)x_i$ denotes the rate at which prey individuals are removed from the system per unit time. It serves as the decision variable for management authorities seeking to balance harvest intensity with population sustainability.

5.3 Objective Functional

We aim to maximize the economic benefits from harvesting prey while accounting for harvesting costs. This trade-off is formulated through the objective functional;

$$J(u) = \int_0^T \sum_{i=1}^{3} \left[\alpha_i u_i(t) x_i(t) - \frac{1}{2} \beta_i u_i^2(t) \right] dt, \tag{5.3}$$

where α_i is the price per unit harvest from patch i, and β_i is a cost coefficient penalizing the harvesting effort. The second term, $\frac{1}{2}\beta_i u_i^2$, is a quadratic cost function representing the increasing marginal cost of harvesting. This structure captures the realistic notion that harvesting costs rise nonlinearly with effort. Economically, the quadratic form ensures diminishing returns on harvesting effort. While higher effort initially yields greater returns, costs eventually outweigh benefits, preventing unrealistic infinite harvesting. This is a standard formulation in bioeconomic and control theory models [20].

5.4 Hamiltonian and Optimality Conditions

To determine the optimal control strategy, we apply Pontryagin's Maximum Principle [20], which provides necessary conditions for optimality in dynamic systems.

Let $\lambda_i(t)$ and $\mu_i(t)$ be the adjoint variables corresponding to $x_i(t)$ and $y_i(t)$, respectively. The Hamiltonian function for the controlled system is defined as;

$$\begin{aligned} H_i = \alpha_i u_i x_i - \frac{1}{2}\beta_i u_i^2 \\ + \lambda_i \left[r_i x_i \left(1 - \frac{x_i}{K_i}\right) - a_i x_i y_i - u_i x_i \right] \\ + \mu_i \left[b_i x_i y_i - d_i y_i \right]. \end{aligned} \tag{5.4}$$

Applying Pontryagin's condition for optimality, the optimal control $u_i^*(t)$ must satisfy;

$$\frac{\partial H_i}{\partial u_i} = 0. \tag{5.5}$$

Differentiating with respect to u_i gives;

$$\frac{\partial H_i}{\partial u_i} = \alpha_i x_i - \beta_i u_i - \lambda_i x_i = 0. \tag{5.6}$$

Solving for u_i yields the unconstrained optimal control;

$$u_i^*(t) = \frac{1}{\beta_i}(\alpha_i - \lambda_i) x_i. \tag{5.7}$$

Since the control is bounded by $0 \leq u_i \leq u_{\max}$, the constrained optimal control becomes;

$$u_i^*(t) = \min\left\{ u_{\max}, \max\left\{ 0, \frac{1}{\beta_i}(\alpha_i - \lambda_i) x_i \right\} \right\}. \tag{5.8}$$

When the prey is abundant and the marginal cost is low ($\lambda_i < \alpha_i$), harvesting effort increases. Conversely, when the prey population declines or the cost of further effort outweighs revenue ($\lambda_i > \alpha_i$), effort decreases toward zero. This dynamic response ensures ecological sustainability and economic efficiency, aligning human exploitation with ecosystem resilience.

5.5 Adjoint Equations

In order to obtain the optimal control formulation, we now obtain the adjoint (or costate) equations, which characterize the behaviour of the shadow prices (marginal values) of the state variables with time. These equations are fundamental aspects of Pontryagin Maximum Principle and make sure that optimality control trajectory obeys biological and economic constraints.

For each patch $i = 1,2,3$, let $\lambda_i(t)$ and $\mu_i(t)$ denote the adjoint variables associated with the prey population $x_i(t)$ and predator population $y_i(t)$, respectively. These adjoint variables measure the sensitivity of the optimal objective functional $J(u)$ to small changes in the corresponding state variables.

According to Pontryagin's Maximum Principle, the adjoint equations are obtained by differentiating the Hamiltonian H_i with respect to the state variables and introducing a negative sign;

$$\frac{d\lambda_i}{dt} = -\frac{\partial H_i}{\partial x_i}, \quad \frac{d\mu_i}{dt} = -\frac{\partial H_i}{\partial y_i}. \tag{5.9}$$

Substituting the Hamiltonian function given by equation (5.4), and differentiating with respect to x_i and y_i gives;

$$\begin{aligned} \frac{d\lambda_i}{dt} &= -\left[\alpha_i u_i - \lambda_i\left(r_i\left(1-\frac{2x_i}{K_i}\right) - a_i y_i - u_i\right) - \mu_i b_i y_i\right], \\ \frac{d\mu_i}{dt} &= \lambda_i a_i x_i + \mu_i(b_i x_i - d_i). \end{aligned} \tag{5.10}$$

These differential equations describe how the marginal value of prey and predator populations evolve over time in response to population dynamics and harvesting effort. The signs and magnitudes of λ_i and μ_i determine whether the system prioritizes prey conservation or immediate economic gain.

The transversality conditions at the terminal time T are given by;

$$\lambda_i(T) = 0, \quad \mu_i(T) = 0. \tag{5.11}$$

which imply that there is no future value assigned to the state variables beyond the management horizon.

The adjoint equations inform valuable insight into sustainable management strategies. A positive $\lambda_i(t)$ indicates that an additional prey individual has a positive marginal value, suggesting that further harvesting may reduce long-term benefits. Conversely, a negative $\lambda_i(t)$ implies that prey are abundant and can be harvested more intensively. Similarly, the term $\mu_i(t)$ reflects the influence of predator abundance on the overall system value where a large positive $\mu_i(t)$ may indicate overpredation risk, necessitating reduced prey harvesting to maintain ecosystem balance.

Figures 5.1 and 5.2 analyze the behavior of the system under optimal harvesting policies, and compare scenarios with and without control.

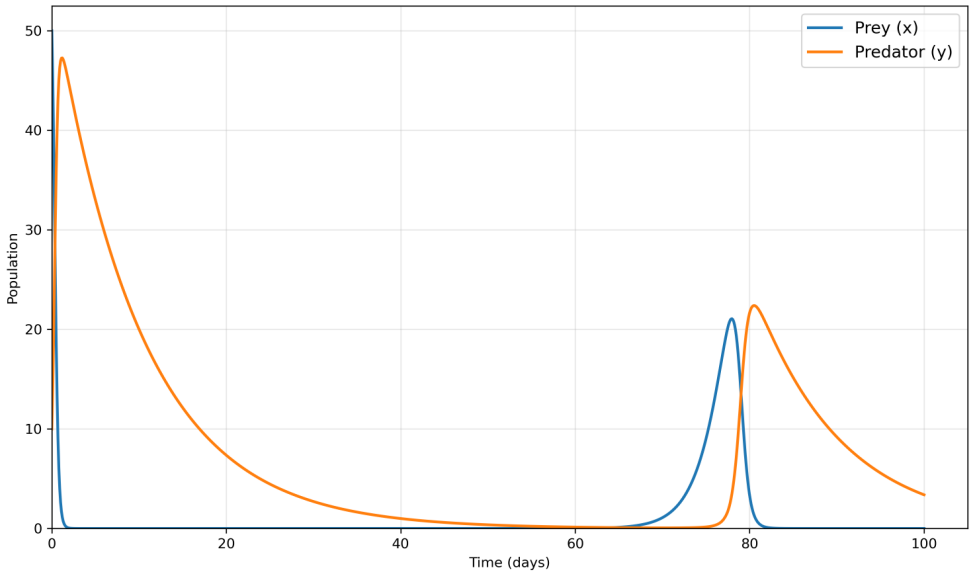

Figure 5.1: Predator-prey Dynamics with constant harvesting efforts.

Figure 5.1 shows how prey and predator populations evolve over time when harvesting is applied at a fixed rate. The prey population declines as a result of constant harvesting and the predator population declines in a similar manner since it is also dependent on the availability of prey that

shows the constraints of constant harvesting of prey in ensuring a long-term ecological balance. Such analysis gives a point where one can compare and see that a more dynamic strategy is needed which is taken into consideration in the optimal control approach.

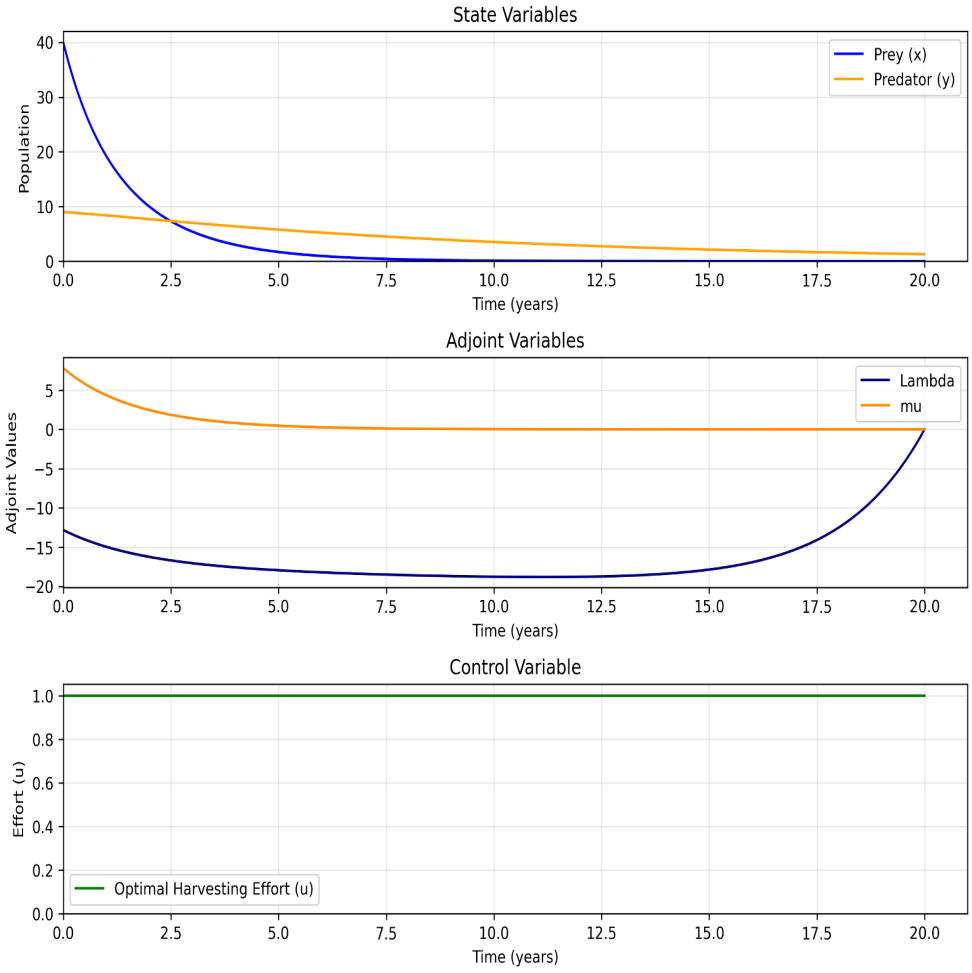

Figure 5.2: Numerical simulation of optimal harvesting.

Figure 5.2 illustrates the dynamics of the predator and prey populations under an optimal harvesting strategy, where the harvesting effort is adjusted over time.

Top plot indicates that the populations are at equilibrium, where the population of the prey are within a sustainable range and payment population of the predators are in response to the change in prey availability.

The intermediate plot is the development of the adjoint variables, the control variables being the

sensitivity of the optimum control to changes in the population of the prey and the predator.

The lower graph illustrates how the optimum level of harvesting work changes with time to ensure the economy and ecology are balanced. The dynamic approach will ensure the long run survival of both populations to avoid overharvesting and will facilitate ecological equilibrium unlike the constant harvesting rate in Figure 5.1.

CHAPTER SIX

NUMERICAL SIMULATION

6.1 Introduction

In this chapter, we investigate the numerical simulation of a stochastic predator-prey model in a three-patch environment to understand the dynamics of interacting species under both deterministic and random influences. In Section 6.2, we present the parameter values used in the model. Section 6.3 explores the time evolution of prey and predator populations in the absence of stochastic effects. Section 6.4 introduces stochasticity into the model and evaluates the effect of varying levels of environmental noise on population dynamics.

For the deterministic model, the system of nonlinear ODEs was solved using the Runge–Kutta method (RK45) [34], implemented through Python software's *solve_ivp()* function. The total simulation time T was divided into small subintervals, and at each step, the population levels of prey (N_i) and predator (M_i) were updated based on the deterministic interactions of growth, predation, mortality, and migration.

For the stochastic model, environmental fluctuations were introduced through random perturbations, and the system was simulated using the Euler–Maruyama scheme [2]. The total simulation time was discretized into small time steps of size Δt, and the populations were updated iteratively as;

$$X_{t+\Delta t} = X_t + f(X_t)\,\Delta t + g(X_t)\,\Delta W_t, \tag{6.1}$$

where $f(X_t)$ represents the deterministic drift term, $g(X_t)$ is the diffusion coefficient that scales the intensity of environmental noise, and $\Delta W_t \sim N(0, \Delta t)$ denotes the Wiener process increment.

6.2 Parameter Values

Table 6.1 represents the corresponding values of our parameters;

Table 6.1: Parameter values

Parameter/Variable	Description	Value	Source
v_1	Harvesting rate in patch 1	0.02	Estimated
v_2	Harvesting rate in patch 2	0.02	Estimated
v_3	Harvesting rate in patch 3	0.02	Estimated
K_1	Carrying capacity of prey species in patch 1	10	Estimated
K_2	Carrying capacity of prey species in patch 2	8	Estimated
K_3	Carrying capacity of prey species in patch 3	6	Estimated
a_1	Predation rate in patch 1	0.2	Estimated
a_2	Predation rate in patch 2	0.3	Estimated
a_3	Predation rate in patch 3	0.4	Estimated
r_1	Intrinsic growth rate of prey in patch 1	0.5	[9]
r_2	Intrinsic growth rate of prey in patch 2	0.4	[9]
r_3	Intrinsic growth rate of prey in patch 3	0.3	[9]
μ_1	Predator death rate in patch 1	0.1	[49]
μ_2	Predator death rate in patch 2	0.1	[49]
μ_3	Predator death rate in patch 3	0.1	[49]
γ_1	Growth rate of predators in patch 1	0.01	Estimated
γ_2	Growth rate of predators in patch 2	0.01	Estimated
γ_3	Growth rate of predators in patch 3	0.01	Estimated
σ_i	Intensity of stochastic fluctuations, $i = 1,2,3$	Variable	Estimated
α_1	Migration rate from patch-1 to patch-2	0.03	Estimated
α_2	Migration rate from patch-2 to patch-3	0.03	Estimated
α_3	Migration rate from patch-3 to patch-1	0.03	Estimated
α_4	Migration rate from patch-2 to patch-1	0.03	Estimated
α_5	Migration rate from patch-3 to patch-2	0.03	Estimated
α_6	Migration rate from patch-1 to patch-3	0.03	Estimated

6.3 Time evaluation of the population without noise.

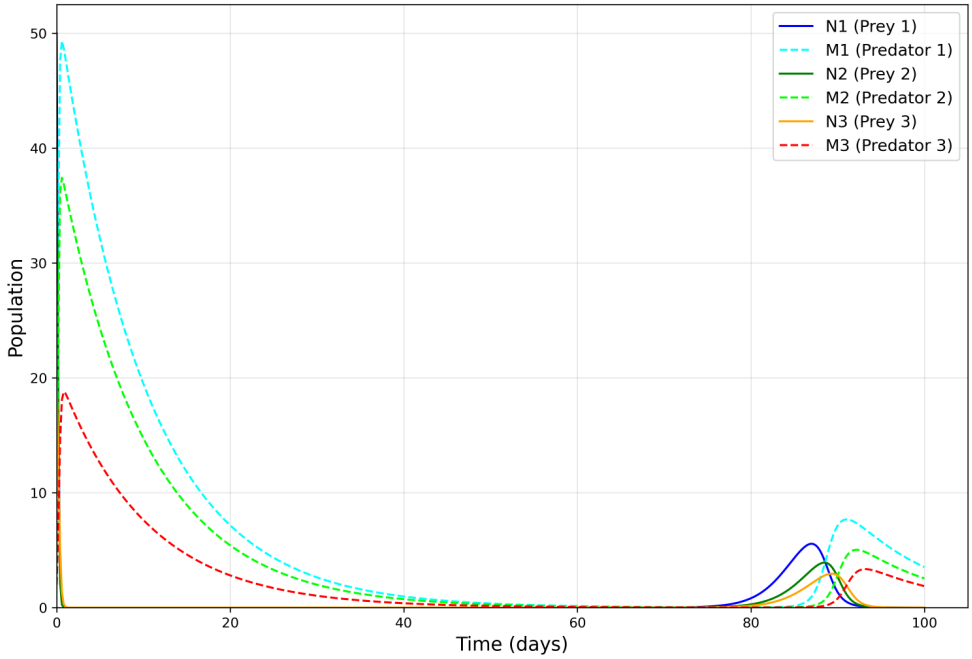

Figure 6.1: Time evaluation of the population $N_1, M_1, N_2, M_2, N_3, M_3$ with initial values 50, 10, 40, 5, 20, 2 respectively.

Figure 6.1 shows the time evaluation of population $N_1, M_1, N_2, M_2, N_3, M_3$ with initial values 50, 10, 40, 5, 20, 2 respectively. Predator populations increase as they feed on the prey, creating predator-prey oscillations. Migration between patches introduces interdependence among the populations, with prey and predators influencing each other's dynamics across the 3 patches. Over time, the populations stabilize reflecting the balance of growth, predation, and migration.

6.4 Stochastic graphs with different additive noise intensities.

The approximations produced by deterministic models are unable to account for the impact of random fluctuations in the environment. We can examine the dynamics of any natural ecosystem that experiences random environmental changes thanks to stochastic analysis. Fish population stochastic graphs produced using Python software for the suggested model with additive noise namely $N_1, M_1, N_2, M_2, N_3, M_3$ in 3 patchy environments are as shown;

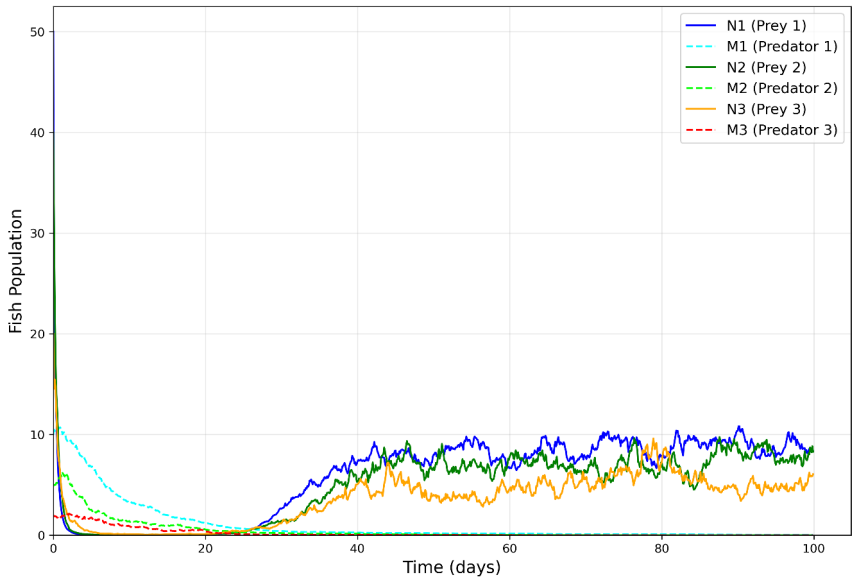

Figure 6.2: Stochastic Dynamics with noise intensities 0.1, 0.05, 0.15, 0.1, 0.2, 0.15 for $N_1, M_1, N_2, M_2, N_3, M_3$ respectively.

Figure 6.2 represents time series evaluation of fish population for the values of noise intensities of 0.1, 0.05, 0.15, 0.1, 0.2, 0.15 for $N_1, M_1, N_2, M_2, N_3, M_3$ respectively. Figure 6.2 clearly shows the little (very less) oscillatory behavior exhibited by all fish population in the three patches, which says model system undergone less influence at these noise intensities (0.1, 0.05, 0.15, 0.1, 0.2, 0.15).

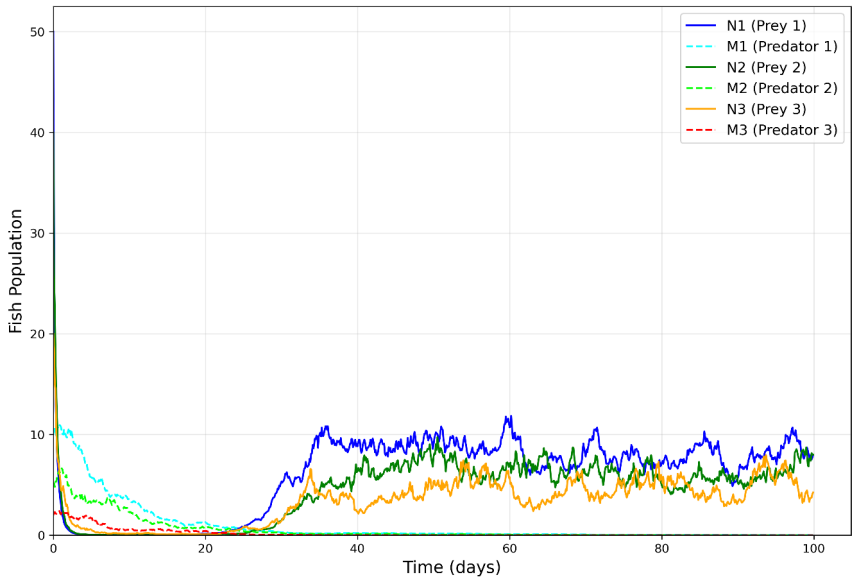

Figure 6.3: Stochastic Dynamics with noise intensities 0.15, 0.1, 0.2, 0.15, 0.25, 0.2 for $N_1, M_1, N_2, M_2, N_3, M_3$ respectively.

Figure 6.3 represents time series evaluation of fish population for the values of noise intensities of 0.15, 0.1, 0.2, 0.15, 0.25, 0.2 for $N_1, M_1, N_2, M_2, N_3, M_3$ respectively. Figure 6.3 clearly shows good oscillatory behavior exhibited by all fish population in the three patches, which says model system undergone great influence at these noise intensities (0.15, 0.1, 0.2, 0.15, 0.25, 0.2).

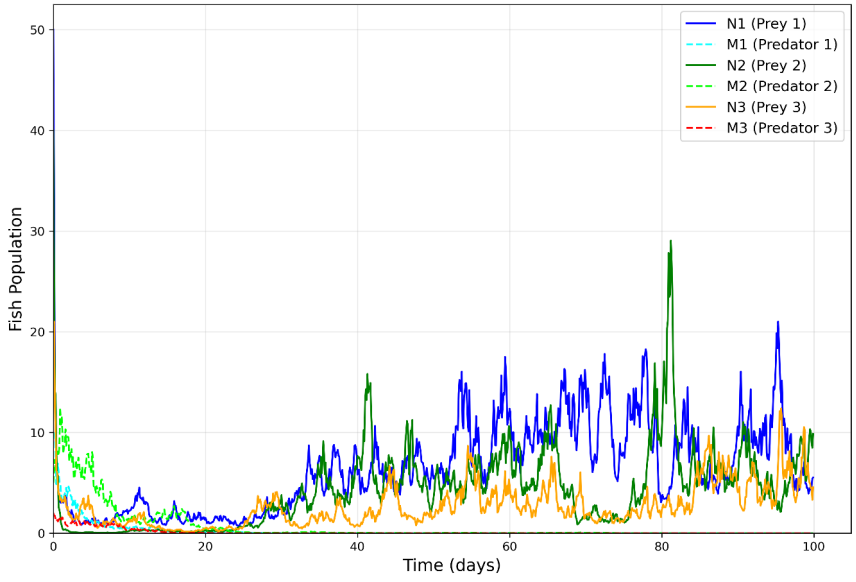

Figure 6.4: Stochastic Dynamics with noise intensities 0.45, 0.4, 0.5, 0.45, 0.55, 0.5 for $N_1, M_1, N_2, M_2, N_3, M_3$ respectively.

Figure 6.4 represents time series evaluation of fish population for the values of noise intensities of 0.45, 0.4, 0.5, 0.45, 0.55, 0.5 for $N_1, M_1, N_2, M_2, N_3, M_3$ respectively. Figure 6.4 clearly shows more oscillatory behavior exhibited by all fish population in the three patches, which says model system undergone great influence at these noise intensities (0.45, 0.4, 0.5, 0.45, 0.55, 0.5).

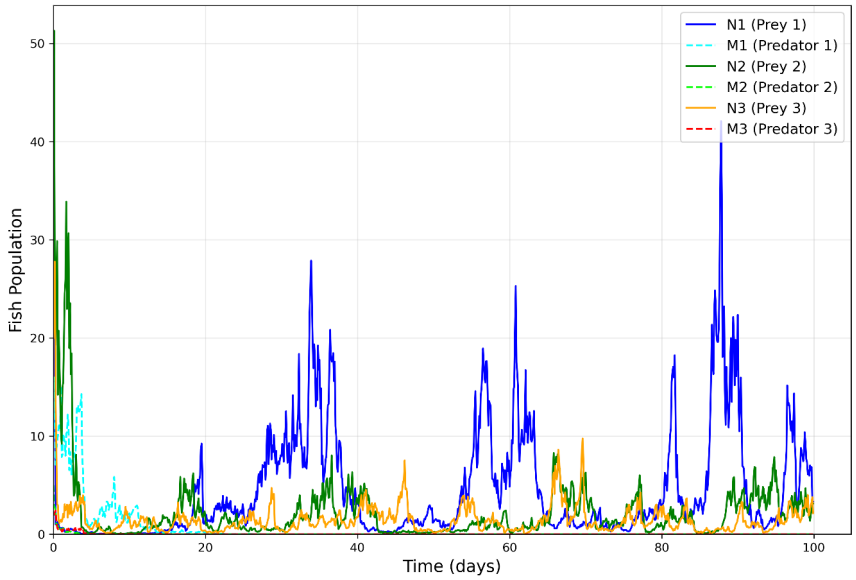

Figure 6.5: Stochastic Dynamics with noise intensities 0.75, 0.8, 0.85, 0.75, 0.9, 0.85 for $N_1, M_1, N_2, M_2, N_3, M_3$ respectively.

Figure 6.5 represents time series evaluation of fish population for the values of noise intensities of 0.75, 0.8, 0.85, 0.75, 0.9, 0.85 for $N_1, M_1, N_2, M_2, N_3, M_3$ respectively. Figure 6.5 clearly shows highly oscillatory behavior exhibited by all fish population in the three patches, which says model system undergone high influence at these noise intensities (0.75, 0.8, 0.85, 0.75, 0.9, 0.85).

The stochastic simulations showed the oscillating populations of prey and predators due to the random disturbances of the environment. At the realistic spectrum of possible noise levels (0.10 0.90), one observed bounded oscillations in the populations, which is a reflection of a dynamic equilibrium between environmental stochasticity and biological control. However, past this threshold, the system was destabilized and population patterns either deviated or collapsed meaning that noise levels that are over-the-top are disequilibrating to the ecological system. These cycles support an ecological understanding of the importance of population viability to stochas-

tic disturbances, especially during periods of low prey density and intense noise responses. The findings highlight the significance of ensuring an environmental variability within manageable margins and adaptive harvesting policies which vary effort with changes in population levels.

CHAPTER SEVEN

CONCLUSION AND RECOMMENDATIONS

7.1 Conclusion

In objective one, the study was to construct a stochastic predator-prey model with optimal harvesting of a three-patch ecosystem to maintain the sustainability of the prey population. The deterministic component of the model was created as a system of Ordinary Differential Equations (ODEs) which was adjusted by adding randomness to reflect environmental variability and uncertainty that was modeled as systems of stochastic differential equations (SDEs), that included the unbounded fluctuations in the population. Some assumptions were also made which explained the various fish populations in the various cages, logistic growth of the prey population and the migration of the fingerlings of the prey which was constant between patches. Migration rates were determined to denote the movement between patches, whereas noise intensities were used to represent the impact of stochastic changes at the hands of both the prey and predator population. It is a broad model that builds upon the existing deterministic models, which provide insights with respect to the dynamics of the ecosystems in complex real-world settings. A three-patch model gives a more realistic model structure, with better representation of spatial heterogeneity and movement between patches, but can still be analysed mathematically and interpreted meaningfully the results of equilibrium and stability.

In objective two, the research did an extensive stability analysis of the deterministic model by analyzing the Jacobian matrix at equilibrium points. It was demonstrated that the trivial equilibrium, $E0$ was a saddle point and therefore unstable, that E1 was locally asymptotically stable, and E2 was revealed to be unstable. The stochastic component of the model was studied with the help of stochastic Lyapunov function method to investigate the impact of environmental variation. The analytic approach was explained using numerical analysis. Based on the results, in

the case where ei is less than 1 (e i is the efficiency of the predator converting prey into a new predator), the lyapunov function V (t) remains finite (decreases as a function of time) showing stochastic stability, and in the case where ei is greater than 1 V (t) increases without bound (drifts upwards with time) showing that the system is unstable. This means that low rates of harvesting or high levels of noise disrupt the system that attaches a premium to the ecological balance mechanism in enforcing harvesting and mortality on the environment, particularly in the face of environmental uncertainty.

In objective three, the investigation sought to come up with the best harvesting policy, which maximizes economic gains, but conservation at an ecological level in a three-patch predator-prey ecosystem. To trade-off between income and the cost of overworking, an objective functional was identified. The Maximum Principle introduced by Pontryagin was used to construct the Hamilton of each patch, resulting in the derivation of conditions that are necessary to be optimal, and the development of an optimal control law. This control law regulates the dynamical energy of the harvesting dynamically to changes in the population and adjoint variables, avoiding an over exploitation of the prey and balancing the predator prey relationship. The result of numerical simulations showed that contrary to constant harvesting strategies, optimal control approach stabilizes population dynamics and leads to long-term sustainability.

Objective four involved the use of numerical simulations to plot the dynamics of the model under different parameter conditions of deterministic and stochastic model dynamics Runge-Kutta method (RK45) and Euler-Maruyama Scheme respectively, with the aid of python software. The simulations validated the theoretical expectations with oscillatory behavior based on rates of harvesting, migration trends, and noise levels. The harvesting rates of prey populations could be kept at an acceptable level (below 0.02, 0.02 and 0.02) and the noise levels kept at 0.10 and 0.90, above which the population became prone to extinction. The discussion has demonstrated how paramount it is to regulate environmental randomness and harvesting actions to stabilize ecological equilibrium.

7.2 Recommendation

The model was only tested on single prey and predator interactions in the three patch ecosystem; thus, further research can diversify the model to incorporate many prey and predator species to better understand the complex food web interactions and inter-species relationships.

REFERENCES

[1] Amar et al., (2024). *Dynamics of a generalist predator–prey system with harvesting and hunting cooperation in deterministic/stochastic environment.* Mathematical Methods in the Applied Sciences. Volume47, Issue7 Pages 5916-5938. https://doi.org/10.1002/mma.9897

[2] Angwenyi, D. (2019). *Time-Continuous State and Parameter Estimation with Application to Hyperbolic SPDEs.* Doctoral thesis, Universität Potsdam, DOI: http://doi.org/10.25932/publishup-43654

[3] Azar, C., Lindgren, K., and Holmberg, J. (1996). *Constant quota versus constant effort harvesting*.

[4] Brauer, F., and Soudack, A. C. (1979). *Stability regions and transition phenomena for harvested predator-prey systems.* Journal of Mathematical Biology 7.4: 319-337.

[5] Brauer, F., and Soudack, A. C. (1981). *Constant-rate stocking of predator-prey systems.* Journal of Mathematical Biology, 11, 1-14.

[6] Brauer, F. (1984). *Constant Yield Harvesting of Population Systems.* In: Levin, S. A., Hallam, T.G. (eds) Mathematical Ecology. Lecture Notes in Biomathematics, vol54. Springer, Berlin, Heidelberg.

[7] Brauer, F., and Chavez, C. C. (2001). *Mathematical models in population biology and epidemiology.* SecondEdition, Springer, New York.

[8] Carroll, C. (2004). *Theoretical foundations of buffer stock saving.* https://doi.org/10.3386/w10867.

[9] Chatterjee, A., and Pal, S. (2023). *A predator-prey model for the optimal control of fish harvesting through the imposition of a tax.* An International Journal

of Optimization and Control: Theories and Applications (IJOCTA), 13(1), 68-80. https://doi.org/10.11121/ijocta.2023.1218

[10] Choirul et al., (2023). *Prey–Predator Mathematics Model for Fisheries Insurance Calculations in the Search of Optimal Strategies for Inland Fisheries Management: A Systematic Literature Review.* Sustainability, 15(16), 12376; https://doi.org/10.3390/su151612376

[11] Darcy et al., (2019). *Opportunities to improve fisheries management through innovative technology and advanced data systems.* Volume20, Issue3, Pages 564-583. https://doi.org/10.1111/faf.12361

[12] Dessy, R. S., Martha, L., and Pratama, R. A. (2023). *Harvesting effect a Ratio-Dependent Predator-Prey Model.* Technium: Romanian Journal of Applied Sciences and Technology, 17(1), 1–7. Retrieved from https://techniumscience.com/index.php/technium/article/view/10038.

[13] Edwige, B., Bernt-Erik, S., and Steinar, E. (2021). *Sustainable strategies for harvesting predators and prey in a fluctuating environment.* Ecological Modelling, Volume 440, 109350. https://doi.org/10.1016/j.ecolmodel.2020.109350.

[14] Hastings, A. (1998). *Population biology, concepts and models.* Springer, New York.

[15] Hiroshi, K. (2010). *Itô's stochastic calculus: Its surprising power for applications, Stochastic Processes and their Applications* Volume 120, Issue 5, Pages 622-652, ISSN 0304-4149, https://doi.org/10.1016/j.spa.2010.01.013.

[16] Jingliang, L.V., and Wang, K. (2011). *Optimal Harvest of a Stochastic Predator-Prey Model.* Hindawi Publishing Corporation Advances in Difference Equations, Volume 2011, Article ID 312465, 18 pages. doi:10.1155/2011/312465.

[17] Joan et al., (2023). *Application of a stochastic compartmental model to approach the spread of environmental events with climatic bias.* Ecological Informatics, Volume 77, 102266.

[18] Kalyan et al., (2015). *Stochastic stability of a fishery model with Optimal Harvesting Policy.* International Journal of Pure and Applied Mathematics, Volume 101 No. 6, 975-983.

[19] Lasse et al., (2011). *The roles of spatial heterogeneity and adaptive movement in stabilizing (or destabilizing) simple metacommunities.* Journal of Theoretical Biology, Volume 291, Pages 76-87.

[20] Lenhart, S. and Workman, J.T. (2007) *Optimal Control Applied to Biological Models.* Mathematical and Computational Biology Series, Chapman and Hall/CRC, London.

[21] Liu, X., and Huang, Q. (2019). *Comparison and analysis of two forms of harvesting functions in the two-prey and one-predator model.* J Inequal, 307.

[22] Lotka, A. J. (1926). *Elements of physical biology.* Elem. Phys. Biol. 82, 341–343.

[23] *Lyapunov's method and the Lasalle invariance principle.* (2023). Ordinary Differential Equations, 79-90. https://doi.org/10.1142/9789811281556-0007.

[24] Mahmud, I. (2021). *Optimal harvesting of a predator-prey system with marine reserve.* Scientific African, Volume 14, e01048.

[25] Mardanov, M. J., and Sharifov, Y. A. (2015). *Pontryagin's maximum principle for the optimal control problems with Multipoint boundary conditions.* Abstract and Applied Analysis, 2015, 1-6. https://doi.org/10.1155/2015/428042.

[26] Mark, K. (2001). *Elements of Mathematical Ecology.* Cambridge University Press, Cambridge, UK. https://doi.org/10.1017/CBO9780511608520.

[27] Meng, L., and Chuanzhi, B. (2014). *Optimal harvesting policy for a stochastic predator–prey model.* Applied Mathematics Letters, Volume 34, Pages 22-26.

[28] Murray, J. D. (2002). *Mathematical biology: I. An introduction.* Third Edition, Springer Verlag, Berlin.

[29] Nadia, M. (2023). *A dynamic analysis of a prey–predator population model with a nonlinear harvesting rate.* Arab Journal of Mathematical Sciences, ISSN: 1319-5166.

[30] Nicholas et al., (2021). *Overfishing drives over one-third of all sharks and rays towards a global extinction crisis.* Current Biology, Volume 31, Issue 21, 4773-4787.

[31] Niranjan, H., Srinivas, M. N., and Viswanathan, K.K. (2023). *Fishery resource management with migratory prey harvesting in two zones- delay and stochastic approach.* Sci Rep;13(1):7273. doi: 10.1038/s41598-023-34130-x. PMID: 37142600; PMCID: PMC10160122.

[32] Pablo, A., Eduardo, G. O., and Soledad, T. (2013). *Stochastic predator–prey model with Allee effect on prey.* Nonlinear Analysis: Real World Applications 14 768–779

[33] Prabir, P., Shyamal, K. M., and Golam, M. (2018). *Dynamics of a predator-prey model with stage-structure on both species and anti-predator behavior.* Volume 10, Pages 50-57, ISSN 2352-9148, https://doi.org/10.1016/j.imu.2017.12.004.

[34] Prince, J., Dormand, R., (1981). it High order embedded Runge-Kutta formulae. Journal of Computational and Applied Mathematics, Volume 7, Issue 1, Pages 67-75, ISSN 0377-0427, https://doi.org/10.1016/0771-050X(81)90010-3.

[35] Sahabuddin, S., Sarijul, I., and Nazmul, S.K. (2023). *Deterministic and stochastic study of an eco-epidemic predator-prey model with nonlinear prey refuge andpredator harvesting.* The European Physical Journal Plus. Volume 138, article number 851.

[36] Sahoo, B., Das B., and Samanta S. (2016). *Dynamics of harvested-predator–prey model: role of alternative resources.* Model. Earth Syst. Environ. 2, 140. https://doi.org/10.1007/s40808-016-0191-x.

[37] Seo, G., DeAngelis, D.L. (2011). *A Predator–Prey Model with a Holling Type I Functional Response Including a Predator Mutual Interference.* J Nonlinear Sci 21, 811–833 (2011). https://doi.org/10.1007/s00332-011-9101-6.

[38] Swapan, C., and Pal, N. B. (2012). *Predator–prey interaction with harvesting: mathematical study with biological ramifications, Applied Mathematical Modelling.* Volume 36, Issue 9, Pages 4044-4059.

[39] Shuai, L., Jin, Z., and Sanling, Y. (2022). *Critical bait casting threshold of cage culture in open advective environments.* Applied Mathematics Letters, Volume 134, 108312.

[40] Syamsuddin, T., and Rustam, T. (2017). *Optimal harvesting policy og predator-prey model with free fishing and reserve zones.* AIP Conference Proceedings 1825, 020023.

[41] Tao, F., Russell, M., and Hao, W. (2023). *Variation in environmental stochasticity dramatically affects viability and extinction time in a predator – prey system with high prey group cohesion.* Mathematical Biosciences 365(39):109075. DOI: 10.1016/j.mbs.2023.109075

[42] Tapan, K. K. (2003). *Selective harvesting in a prey-predator fishery with time delay.* Mathematical and Computer Modelling, vol. 38, no. 3-4, pp. 449–458.

[43] Tapan, K. K. and Pahari, U. K. (2007). *Modelling and analysis of a prey-predator system with stage-structure and harvesting.* Nonlinear Analysis. Real World Applications, vol. 8, no. 2, pp. 601–609.

[44] Tapan, K. K. and Chakraborty, K. (2010). *Effort dynamic in a prey-predator model with harvesting.* International Journal of Information and Systems Sciences, vol. 6, no. 3, pp. 318–332.

[45] Tapan, K. K. and Ghorai, A. (2011). *Dynamic behaviour of a delayed predators-prey model with harvesting.* Applied Mathematics and Computation, vol. 217, no. 22, pp. 9085–9104.

[46] Tapan, K. K. (2006). *Modelling and analysis of a harvested prey–predator system incorporating a prey refuge.* Journal of Computational and Applied Mathematics, Volume 185, Issue 1, Pages 19-33.

[47] Ugo, B., Mario, S., and Dominique, S. (2021). *Introduction to the Pontryagin Maximum Principle for Quantum Optimal Control.* PRX Quantum. DOI: https://doi.org/10.1103/PRXQuantum.2.030203.

[48] Volterra, V. (1926). *Variazioni e fluttuazioni del numero d'individui in specie animali conviventi.* In Memoire della Real Accademia Nazionale dei Lincei II; Rome, Italy; pp. 31–113.

[49] Wang, J., and Nie, H. (2022). *Invasion dynamics of a predator-prey system in closed advective environments.* Journal of Differential Equations, 318, 298-322. https://doi.org/10.1016/j.jde.2022.02.043

[50] Wedig, W. V. (2020). *Lyapunov exponents of stochastic systems and related bifurcation problems.* Stochastic Structural Dynamics, 315-327. https://doi.org/10.1201/9781003076582-16

[51] Yousef, A., and Moustafa, E. (2022). *Deterministic and Stochastic Prey–Predator Model for Three Predators and a Single Prey.* Axioms, 11(4), 156; https://doi.org/10.3390/axioms11040156.

[52] Yunfei, L.V., Rong Y., and Yongzhen P. (2012). *A prey-predator model with harvesting for fishery resource with reserve area.* Applied Mathematical Modelling, Volume 37, Issue 5, Pages 3048-3062, https://doi.org/10.1016/j.apm.2012.07.030.

APPENDIX

Appendix A: Python Code to generate figure 6.1

```
#!/usr/bin/env python
# coding: utf-8

# In[2]:


import matplotlib.pyplot as plt
import pandas as pd
import numpy as np
import scipy as sp
from scipy.integrate import solve_ivp


# In[3]:


# Hypothetical parameter values
params = {
    'r1': 0.5, 'r2': 0.4, 'r3': 0.3,        # Growth rates
    'K1': 10, 'K2': 8, 'K3': 6,             # Carrying capacities
    'a1': 0.2, 'a2': 0.3, 'a3': 0.4,        # Interaction coefficients
    'mu1': 0.1, 'mu2': 0.1, 'mu3': 0.1,     # Death rates of M
    'gamma3': 0.01,                         # Interaction rates (N to M)
    'alpha1': 0.03, 'alpha2': 0.03, 'alpha3': 0.03, # Loss rates for N
    'alpha4': 0.03, 'alpha5': 0.03, 'alpha6': 0.03
}


# In[4]:

```

```
31
32 # System of differential equations
33 def model(t, y, params):
34     N1, M1, N2, M2, N3, M3 = y
35
36     r1, r2, r3 = params['r1'], params['r2'], params['r3']
37     K1, K2, K3 = params['K1'], params['K2'], params['K3']
38     a1, a2, a3 = params['a1'], params['a2'], params['a3']
39     mu1, mu2, mu3 = params['mu1'], params['mu2'], params['mu3']
40     gamma3 = params['gamma3']
41     alpha1, alpha2, alpha3 = params['alpha1'], params['alpha2'], params['
    alpha3']
42     alpha4, alpha5, alpha6 = params['alpha4'], params['alpha5'], params['
    alpha6']
43
44     dN1_dt = r1 * N1 * (1 - N1 / K1) - a1 * M1 * N1 + alpha4 * N2 +
    alpha5 * N3 - (alpha6 + alpha3) * N1
45     dM1_dt = a1 * M1 * N1 - mu1 * M1
46     dN2_dt = r2 * N2 * (1 - N2 / K2) - a2 * M2 * N2 + alpha1 * N1 +
    alpha5 * N3 - (alpha2 + alpha6) * N2
47     dM2_dt = a2 * M2 * N2 - mu2 * M2
48     dN3_dt = r3 * N3 * (1 - N3 / K3) - a3 * M3 * N3 + alpha1 * N1 +
    alpha2 * N2 - (alpha3 + alpha5) * N3
49     dM3_dt = a3 * M3 * N3 - mu3 * M3
50
51     return [dN1_dt, dM1_dt, dN2_dt, dM2_dt, dN3_dt, dM3_dt]
52
53
54 # In[5]:
55
56
57 # Initial conditions
58 y0 = [50, 10, 40, 5, 20, 2]  # Initial populations for N1, M1, N2, M2, N3
    , M3
```

```
59
60
61 # In[6]:
62
63
64 # Time span for simulation
65 t_span = (0, 100)  # Simulate from day 0 to day 100
66 t_eval = np.linspace(t_span[0], t_span[1], 500)  # 500 points for smooth
       curve
67
68
69 # In[7]:
70
71
72 # Solve the system numerically
73 solution = solve_ivp(model, t_span, y0, args=(params,), t_eval=t_eval,
       method='RK45')
74
75
76 # In[8]:
77
78
79 # Extract results
80 t = solution.t
81 N1, M1, N2, M2, N3, M3 = solution.y
82
83
84 # In[9]:
85
86
87 # Plot the dynamics of all populations
88 plt.figure(figsize=(12, 8))
89
90 plt.plot(t, N1, label='N1 (Prey 1)', color='blue')
```

```
plt.plot(t, M1, label='M1 (Predator 1)', color='cyan', linestyle='--')
plt.plot(t, N2, label='N2 (Prey 2)', color='green')
plt.plot(t, M2, label='M2 (Predator 2)', color='lime', linestyle='--')
plt.plot(t, N3, label='N3 (Prey 3)', color='orange')
plt.plot(t, M3, label='M3 (Predator 3)', color='red', linestyle='--')

plt.title('Time Series Evaluation of the Population', fontsize=16)
plt.xlabel('Time (days)', fontsize=14)
plt.ylabel('Population', fontsize=14)

# Remove extra space so axes start exactly at (0,0)
plt.xlim(left=0)
plt.ylim(bottom=0)

# Add grid and legend (key)
plt.grid(alpha=0.3)
plt.legend(loc='upper right', fontsize=12, frameon=True)

# Save the figure as PNG (high resolution)
plt.savefig("a5.png", dpi=300, bbox_inches='tight')

# Tighten layout for a clean look
plt.tight_layout(pad=0)

plt.show()
```

Appendix B: Python Code to generate figure 6.2

```
#!/usr/bin/env python
# coding: utf-8

# In[10]:


import matplotlib.pyplot as plt
```

```
import pandas as pd
import numpy as np
import scipy as sp


# In[11]:


# Hypothetical parameter values
params = {
    'r1': 0.5, 'r2': 0.4, 'r3': 0.3,        # Growth rates
    'K1': 10, 'K2': 8, 'K3': 6,             # Carrying capacities
    'a1': 0.2, 'a2': 0.3, 'a3': 0.4,        # Interaction coefficients
    'mu1': 0.1, 'mu2': 0.1, 'mu3': 0.1,     # Death rates of M
    'gamma1': 0.01, 'gamma2': 0.01, 'gamma3': 0.01, # Interaction rates (
   N to M)
    'alpha1': 0.03, 'alpha2': 0.03, 'alpha3': 0.03,
    'alpha4': 0.03, 'alpha5': 0.03, 'alpha6': 0.03, # Loss rates
    'nu1': 0.02, 'nu2': 0.02, 'nu3': 0.02, # Removal rates
    # Noise intensities for each patch
      'sigma1_N': 0.1, 'sigma1_M': 0.05,    # Patch 1
      'sigma2_N': 0.15, 'sigma2_M': 0.1,    # Patch 2
      'sigma3_N': 0.2, 'sigma3_M': 0.15     # Patch 3
}


# In[12]:


# Initial populations
y0 = [50, 10, 40, 5, 20, 2]  # Initial populations for N1, M1, N2, M2, N3
   , M3


```

```
# In[13]:


# Time parameters
t_start, t_end, dt = 0, 100, 0.1  # Simulation from t=0 to t=100, step=0.1
time = np.arange(t_start, t_end, dt)
num_steps = len(time)


# In[14]:


# Initialize population arrays
states = np.zeros((num_steps, len(y0)))
states[0, :] = y0


# In[15]:


# Function to compute deterministic part
def deterministic_part(y, params):
    N1, M1, N2, M2, N3, M3 = y

    r1, r2, r3 = params['r1'], params['r2'], params['r3']
    K1, K2, K3 = params['K1'], params['K2'], params['K3']
    a1, a2, a3 = params['a1'], params['a2'], params['a3']
    mu1, mu2, mu3 = params['mu1'], params['mu2'], params['mu3']
    gamma1, gamma2, gamma3 = params['gamma1'], params['gamma2'], params['gamma3']
    alpha1, alpha2, alpha3 = params['alpha1'], params['alpha2'], params['alpha3']
    alpha4, alpha5, alpha6 = params['alpha4'], params['alpha5'], params['
```

```
    alpha6']
71      nu1, nu2, nu3 = params['nu1'], params['nu2'], params['nu3']
72
73      dN1_dt = r1 * N1 * (1 - N1 / K1) - a1 * N1 * M1 - nu1 * N1 + alpha4 *
        N2 + alpha3 * N3 - (alpha1 + alpha6) * N1
74      dM1_dt = gamma1 * N1 * M1 - mu1 * M1 - nu1 * M1
75      dN2_dt = r2 * N2 * (1 - N2 / K2) - a2 * N2 * M2 - nu2 * N2 + alpha1 *
        N1 + alpha5 * N3 - (alpha2 + alpha4) * N2
76      dM2_dt = gamma2 * N2 * M2 - mu2 * M2 - nu2 * M2
77      dN3_dt = r3 * N3 * (1 - N3 / K3) - a3 * N3 * M3 - nu3 * N3 + alpha2 *
        N2 + alpha6 * N1 - (alpha3 + alpha5) * N3
78      dM3_dt = gamma3 * N3 * M3 - mu3 * M3 - nu3 * M3
79
80      return np.array([dN1_dt, dM1_dt, dN2_dt, dM2_dt, dN3_dt, dM3_dt])
81
82
83  # In[16]:
84
85
86  # Simulate using Euler-Maruyama method
87  for i in range(1, num_steps):
88      current_state = states[i - 1, :]
89      noise = np.array([
90          params['sigma1_N'] * current_state[0] * np.random.normal(0, np.
    sqrt(dt)),  # Noise for N1
91          params['sigma1_M'] * current_state[1] * np.random.normal(0, np.
    sqrt(dt)),  # Noise for M1
92          params['sigma2_N'] * current_state[2] * np.random.normal(0, np.
    sqrt(dt)),  # Noise for N2
93          params['sigma2_M'] * current_state[3] * np.random.normal(0, np.
    sqrt(dt)),  # Noise for M2
94          params['sigma3_N'] * current_state[4] * np.random.normal(0, np.
    sqrt(dt)),  # Noise for N3
95          params['sigma3_M'] * current_state[5] * np.random.normal(0, np.
```

```
    sqrt(dt))   # Noise for M3
     ])
     deterministic_change = deterministic_part(current_state, params) * dt
     states[i, :] = current_state + deterministic_change + noise


# In[17]:


# Extract results
N1, M1, N2, M2, N3, M3 = states.T


# In[18]:


# Plot results
plt.figure(figsize=(12, 8))
plt.plot(time, N1, label='N1 (Prey 1)', color='blue')
plt.plot(time, M1, label='M1 (Predator 1)', color='cyan', linestyle='--')
plt.plot(time, N2, label='N2 (Prey 2)', color='green')
plt.plot(time, M2, label='M2 (Predator 2)', color='lime', linestyle='--')
plt.plot(time, N3, label='N3 (Prey 3)', color='orange')
plt.plot(time, M3, label='M3 (Predator 3)', color='red', linestyle='--')
plt.title('Stochastic Dynamics with noise intensities', fontsize=16)
plt.xlabel('Time (days)', fontsize=14)
plt.ylabel('Fish Population', fontsize=14)
plt.legend(fontsize=12)
plt.grid(alpha=0.3)

# Remove extra space so axes start exactly at (0,0)
plt.xlim(left=0)
plt.ylim(bottom=0)

```

```
# Add grid and legend (key)
plt.grid(alpha=0.3)
plt.legend(loc='upper right', fontsize=12, frameon=True)

# Save the figure as PNG (high resolution)
plt.savefig("a6.png", dpi=300, bbox_inches='tight')

# Tighten layout for a clean look
plt.tight_layout(pad=0)
plt.show()
```